

## Supplementary Material

# Synthesis of Thermo-Shear-Responsive Dynamic Covalent Networks based on Humins and the Diels-Alder Reaction

Dilhan Kandemir<sup>[a]</sup>, Meghana Mekala<sup>[b]</sup>, Ruth Cardinaels<sup>[b]</sup>, Peter Van Puyvelde<sup>[b]</sup>, Anton Ginzburg<sup>\*[a]</sup>

[a] Dilhan Kandemir, Anton Ginzburg

Department of Chemical Engineering, Soft Matter, Rheology and Technology

KU Leuven,

Wetenschapspark 27, 3590 Diepenbeek, Belgium.

E-mail: anton.ginzburg@kuleuven.be

[b] Meghana Mekala, Ruth Cardinaels, Peter Van Puyvelde

Department of Chemical Engineering, Soft Matter, Rheology and Technology

KU Leuven

Celestijnenlaan 200J, 3001 Heverlee, Belgium.

## General Information

**Chemicals:** Humins (New Batch, GEBR194, GEBR190, BR236) were kindly provided by Avantium Renewable Chemicals BV and used as received. 1,1'-(Methylenedi-4,1-phenylene)bismaleimide (95%, Sigma-Aldrich), acetyl chloride (98%, Sigma-Aldrich), adipoyl chloride (98%, Sigma-Aldrich), benzoyl chloride (99%, Sigma-Aldrich), furfuryl alcohol (for synthesis, Sigma-Aldrich), triethylamine (Et<sub>3</sub>N, 99%, Sigma-Aldrich), poly(propylene glycol) bis(2-aminopropyl ether) (Sigma-Aldrich), BMI1500 (Sigma-Aldrich). Tetrahydrofuran (THF, 99%, Sigma-Aldrich) and dichloromethane (DCM, 99%, Sigma-Aldrich) were HPLC grade and used without further purification. All other chemicals were used as received.

**Fourier Transform Infrared Spectroscopy (FTIR):** A Perkin Elmer Spectrum 65 FT-IR spectrometer equipped with a Perkin Elmer (Waltham, United States) universal attenuated total reflection (ATR) accessory and pressure arm was used to collect spectra from 4000 cm<sup>-1</sup> to 600 cm<sup>-1</sup> for each sample at room temperature. The resolution of the instrument was set at 0.5 cm<sup>-1</sup>. Before each measurement, the ATR diamond crystal was cleaned with acetone, and a background scan was performed between each sample. Subsequently, the collected spectra were analysed using the accompanying Perkin-Elmer software. For semi-quantitative analysis of the furanic content, all spectra were converted to absorbance and normalised using a reference band to account for variations in sample contact and effective path length. Specifically, the absorbance at 1025 cm<sup>-1</sup>, assigned to the C-O-C stretching vibration of the furan ring, was used as the analytical band. Calibration curves were established using furfuryl alcohol (FA) and Humins1 solutions in THF (10-50 mg mL<sup>-1</sup>), and the furan content of humins was determined by comparing the normalised absorbance values at 1025 cm<sup>-1</sup>.

**Nuclear Magnetic Resonance (NMR):** High-field nuclear magnetic resonance (NMR) spectra were recorded on a Bruker Avance II+ 600 spectrometer with a Bruker 600 UltraShield<sup>TM</sup> magnet system (<sup>1</sup>H fundamental frequency of 600.13 MHz) and a 5 mm PABBO BB-<sup>1</sup>H/D probe with z-gradients. All samples were dissolved in DMSO-d<sub>6</sub>. Data were recorded at room temperature using Bruker TopSpin 3.6.x software. The δ-values are expressed in parts per million (ppm). The following acronyms were used: s (singlet), d (doublet), t (triplet), m (multiplet), br (broadened).

<sup>1</sup>H NMR spectra of the humins batches were recorded in DMSO-d<sub>6</sub> to examine the presence of furan-derived structural motifs prior to Diels-Alder network formation. Samples were prepared by dissolving Humins1 (16 mg), Humins2 (14 mg), Humins3 (17 mg), and Humins4 (16 mg) in 0.5 mL of DMSO-d<sub>6</sub>, resulting in concentrations that enable relative comparison of spectral features across the humins batches. For comparative purposes, the aromatic/furanic region of the spectra (6.4-7.6 ppm) was evaluated at an estimation level (Table S2).

**Rheological Characterisation:** Rheological tests were conducted using an Anton Paar MCR 302e (Graz, Austria), employing linear viscoelastic measurements. The rheometer was equipped with an ETD heating system and operated under a nitrogen atmosphere. All materials were characterised using a 25 mm diameter parallel-plate geometry with a 1 mm gap. Amplitude sweep tests were performed over a strain range of 0.01–100 % at a fixed frequency of 1 Hz to determine the linear viscoelastic region (LVE). Depending on the material, the LVE was typically found to be below 0.5–1% strain. Frequency sweep experiments were conducted within the LVE at a strain amplitude of 1 %, with frequencies ranging from 100 to 0.1 Hz. Time- and temperature-dependent oscillatory shear experiments were performed within the LVE using multiple combinations of strain amplitude and frequency, depending on the experiment, including 0.1% to 1% strain and 1 to 50 Hz frequency, with temperatures varying up to 100 °C. All temperature ramps were applied at a heating rate of 2 °C min<sup>-1</sup>, unless stated otherwise. Frequencies are reported in Hz throughout the Supplementary Information ( $\omega = 2\pi f$ ).

**Thermogravimetric analysis (TGA):** TGA was performed on a Netzsch STA 449 F3 Jupiter instrument (Selb, Germany) in a synthetic air atmosphere (80% nitrogen/20% oxygen) flowing at a rate of 50 mL/min. After the TGA chamber was purged, approximately 10-15 mg of samples in alumina crucibles were heated to 550 °C at a rate of 10 °C/min. To compensate for the buoyancy effect, the weight reduction of an empty crucible under the same conditions was subtracted from the measured data.

**Dielectric setup:** The electrical conductivity of pure humins and humins after undergoing the Diels-Alder reaction was measured at room temperature (20°C) and 60°C using a rheo-dielectric setup. The setup consisted of a dielectric analyser (Novocontrol Technologies, Montabaur, Germany), paired with an MCR501 stress-controlled rheometer (Anton Paar, Graz, Austria), and a CTD450 temperature-controlled convection oven operated under a nitrogen atmosphere. Dielectric measurements were conducted with the rheometer plates serving as electrodes. The bottom plate had a diameter of 25 mm, and a disposable PP25 geometry was used as the top plate. The gap height between the plates was constant at approximately 1 mm for all samples. Conductivity spectroscopy was performed over a frequency range of 10<sup>-2</sup> to 10<sup>7</sup> Hz, and the real part of the conductivity was reported.

**General Procedure for Furfuryl Alcohol Bismaleimide Model Reaction:** Furfuryl alcohol (1.0 g, 10.2 mmol) was dissolved in tetrahydrofuran (THF, 20 mL) in a 50 mL round-bottom flask under stirring at room temperature. To this solution, 1,1'-(Methylenedi-4,1-phenylene)bismaleimide (5.1 mmol, equimolar maleimide groups relative to furfuryl alcohol) was added gradually to ensure thorough mixing. The reaction mixture was then stirred at room temperature for 72 hours. The reaction was stopped upon completion, and the resulting mixture was transferred to a sample vessel, where it was left to dry in a fume hood under ambient conditions.

**General Procedure for Humins Diels Alder Adducts:** Humins (2.25 g) were dissolved in tetrahydrofuran (THF, 30 mL) at room temperature in a 50 mL round-bottom flask. The mixture was stirred for 15 minutes until the humins were completely dissolved. Subsequently, 1,1'-(Methylenedi-4,1-phenylene)bismaleimide (0.75 g) was added as a solid to the flask. The reaction mixture was stirred continuously for three days at room temperature. After three days, the reaction was stopped, and the resulting mixture was transferred to a sample vessel, where it was left to dry in a fume hood under ambient conditions.

**General Procedure for Post-Treatment with PPG-diamine:** Humins–BMI Diels–Alder adduct (3.00 g, solid) was dissolved in tetrahydrofuran (THF, 25 mL) at room temperature in a 50 mL round-bottom flask. Poly(propylene glycol) bis(2-aminopropyl ether) (PPG-diamine,  $M_n \approx 2000 \text{ g mol}^{-1}$ ) was added neat in an amount corresponding to 0.5–1.0 equiv of –NH<sub>2</sub> per maleimide double bond. The reaction mixture was stirred at room temperature for 12 h, followed by gentle heating at 40–50 °C for an additional 1–2 h to ensure complete homogenization. The solvent was removed under reduced pressure at a temperature of  $\leq 40 \text{ °C}$ , affording a putty-like material that was used as obtained for subsequent rheological measurements. This post-treatment step is intended to selectively consume residual maleimide double

bonds via aza-Michael addition, thereby suppressing further DA-related crosslinking and stabilising the material in a putty-like state.

Throughout this work, the terms 'putty-like' and 'solid' are used to distinguish intermediate viscoelastic states governed by DA equilibrium evolution rather than compositional differences.

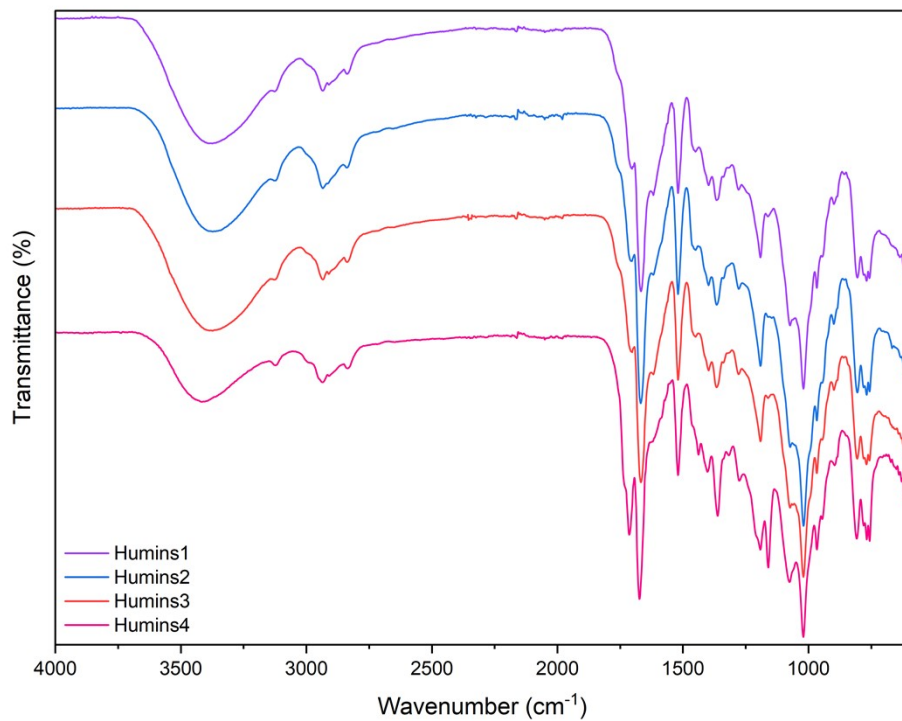


**Figure S1.** ATR-FTIR spectra of four different industrial humins samples.

**Table S1.** <sup>1</sup>H NMR data for humins samples Humins1-4 (600 MHz, DMSO-d<sub>6</sub>, 25 °C).

$\delta$ (ppm)	Multiplicity <sup>1</sup>	Assignment	Observed in samples <sup>2</sup>	Comment
9.8–8.5	br s / br m	Aldehydic/formyl protons (–CHO)	Humins1-4	Weak, broad signals; indicative of terminal oxidised motifs.
8.5–7.5	br m	Aromatic/oxidised furanic protons	Humins1-4	Part of the main aromatic/furanic envelope.
7.5–6.0	br m	Furanic and other aromatic protons	Humins1-4	Dominant broad hump; characteristic of humin cores.
6.2–5.4	br m	Vinylic/conjugated C=C–H	Humins1-4 (weak)	Often appears as shoulders in the aromatic region.
5.4–4.5	br m	O–CH / acetal-like protons	Humins1-4	Broad, unresolved; likely acetal/ether/ester environments.
4.5–4.0	br m	O–CH, O–CH <sub>2</sub> adjacent to oxygenated centres	Humins1-4	Overlaps with other O–CH regions; no resolved multiplicity.
4.0–3.0	br m	CH–O, CH <sub>2</sub> –O in polyether/ester fragments	Humins1-4	Intense, broad envelope; typical for oxygen-rich side chains.
3.0–2.2	br m	Aliphatic CH / CH <sub>2</sub> next to C=O or aromatics	Humins1-4	Includes benzylic / $\alpha$ -CO protons; partially overlaps with DMSO (2.50).
2.2–1.5	br m	Saturated CH <sub>2</sub> /CH groups in the humin backbone	Humins1-4	Broad hump, no resolved pattern.
1.5–0.5	br m	Terminal CH <sub>3</sub> and other aliphatic groups	Humins1-4	Low-intensity, very broad; consistent with aliphatic chain ends.

<sup>1</sup>H NMR spectra of all humins batches (Humins1-4) display very broad, heavily overlapping resonances due to their intrinsic structural heterogeneity. Therefore, only chemical shift ranges and qualitative signal families are reported. Accurate integrals and coupling constants (J) cannot be reliably extracted and are not given.

<sup>1</sup> br s = broad singlet; br m = broad multiplet. Multiplicities are purely descriptive, as individual spin systems cannot be resolved due to extensive overlap and line broadening.

<sup>2</sup> All humins samples (Humins1–4) show qualitatively similar patterns; only minor relative intensity differences are observed between batches.

**Table S2.** Sample preparation conditions and estimation-level comparison of the aromatic/furanic region in the <sup>1</sup>H NMR spectra of the humins batches.

Sample	Mass (mg)	Concentration (mg/mL)	Normalisation factor*	Furanic region integral (6.2-7.6 ppm)**	Normalised furanic integral
Humins1	11	22	1.455	13.72	19.96
Humins2	14	28	1.143	34.93	39.92
Humins3	17	34	0.941	24.40	22.96
Humins4	16	32	1.000	43.74	43.74

\* Normalisation factor corrects for minor differences in sample concentration in 0.5 mL DMSO-d<sub>6</sub> and was calculated relative to the concentration of 32 mg/mL.

\*\* Furanic region integral corresponds to concentration normalised integration of the aromatic/furanic region and is used only for relative comparison between batches.

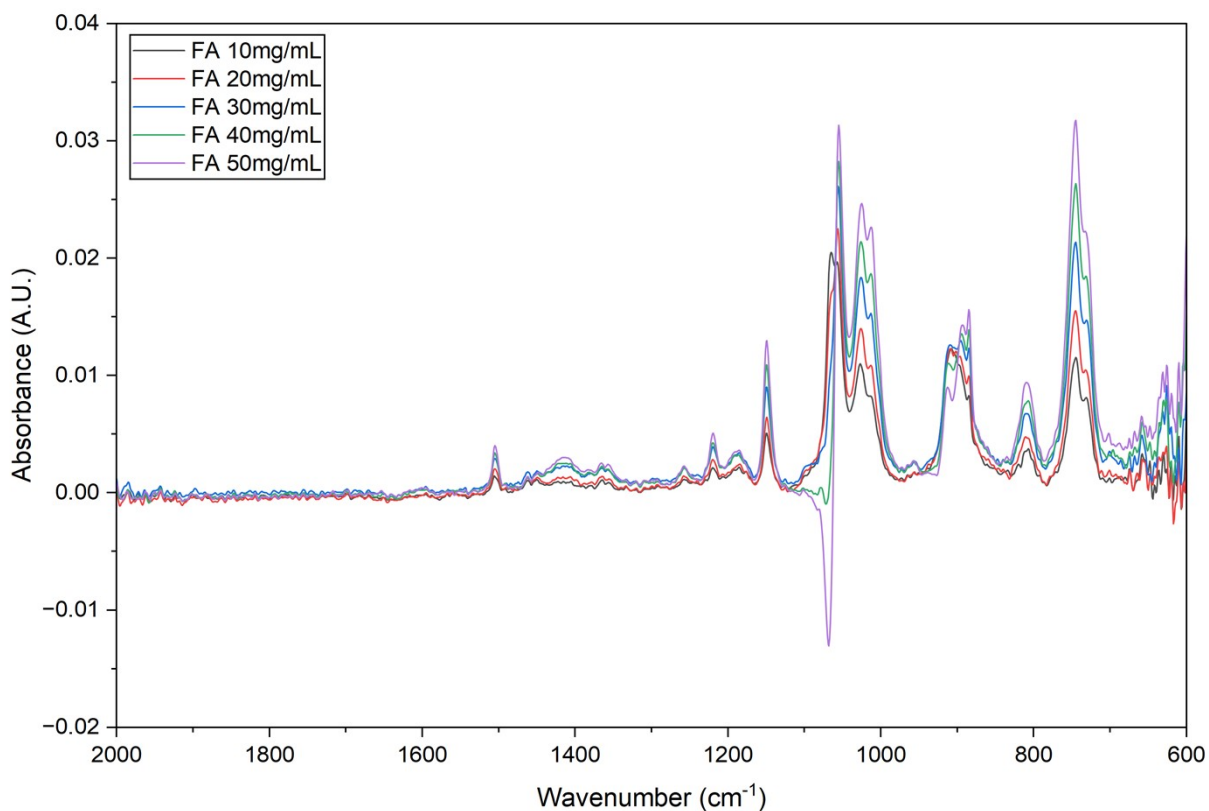


**Figure S2.** ATR-FTIR spectrum of a calibration study with furfuryl alcohol.

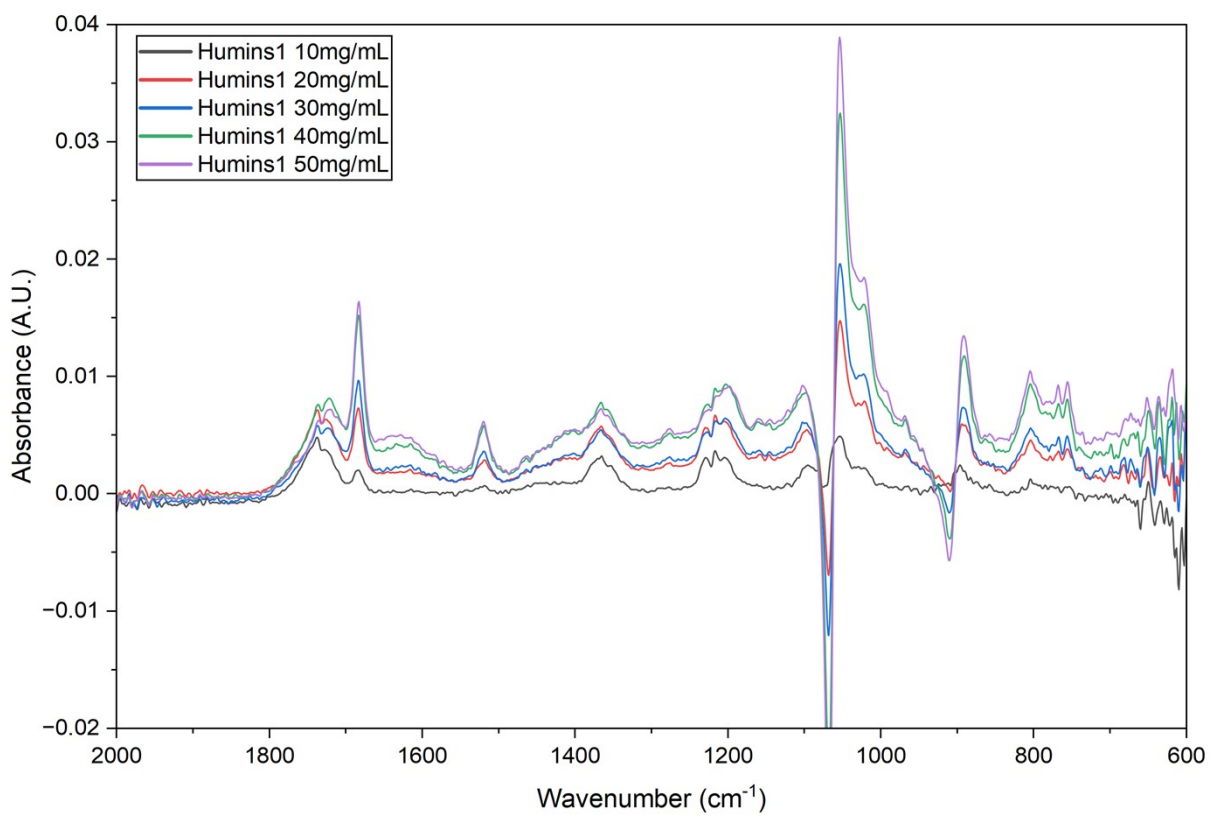


**Figure S3.** ATR-FTIR spectrum of a calibration study with Humins1.

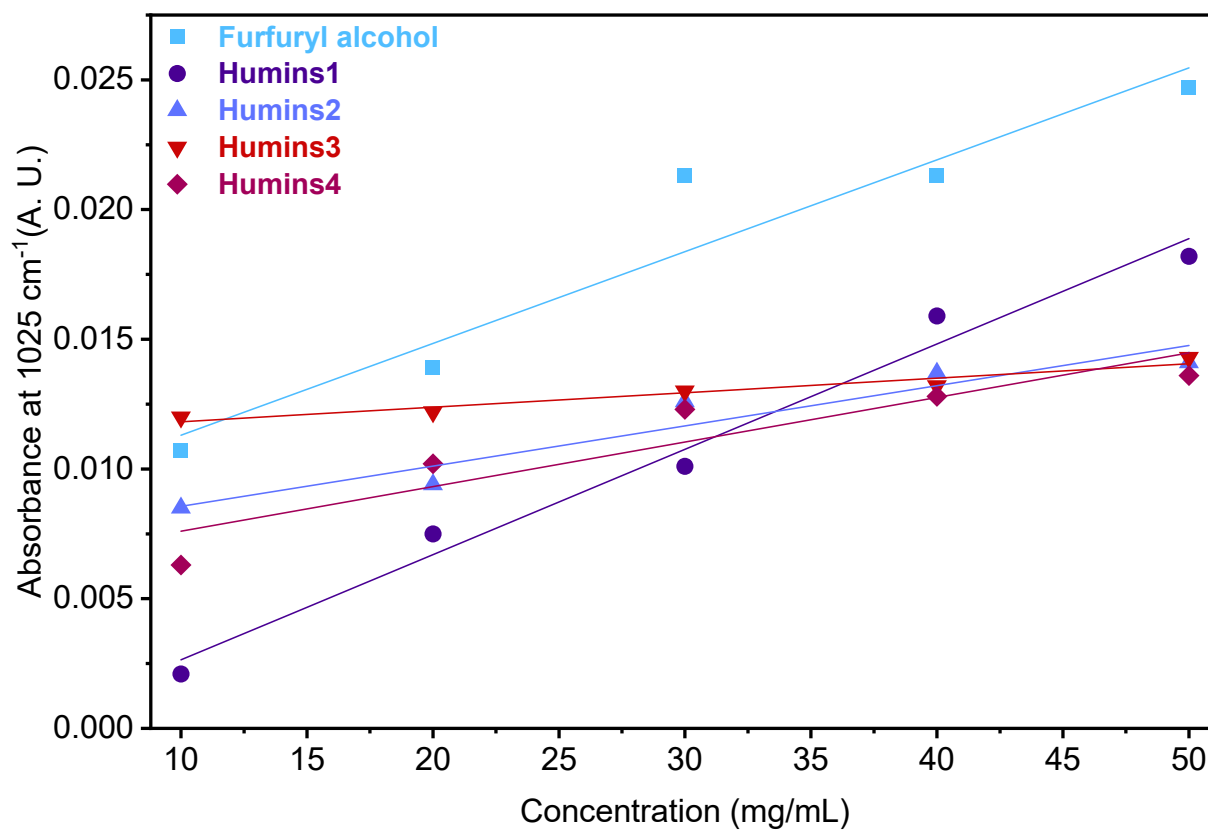


**Figure S4.** FTIR calibration curve used to semi-quantify the furanic content of humins, based on ATR-IR spectra of furfuryl alcohol (FA) and Humins1-4 THF solutions (10-50 mg mL<sup>-1</sup>) monitored at 1025 cm<sup>-1</sup> (C-O-C stretch of furan ring) in absorbance.

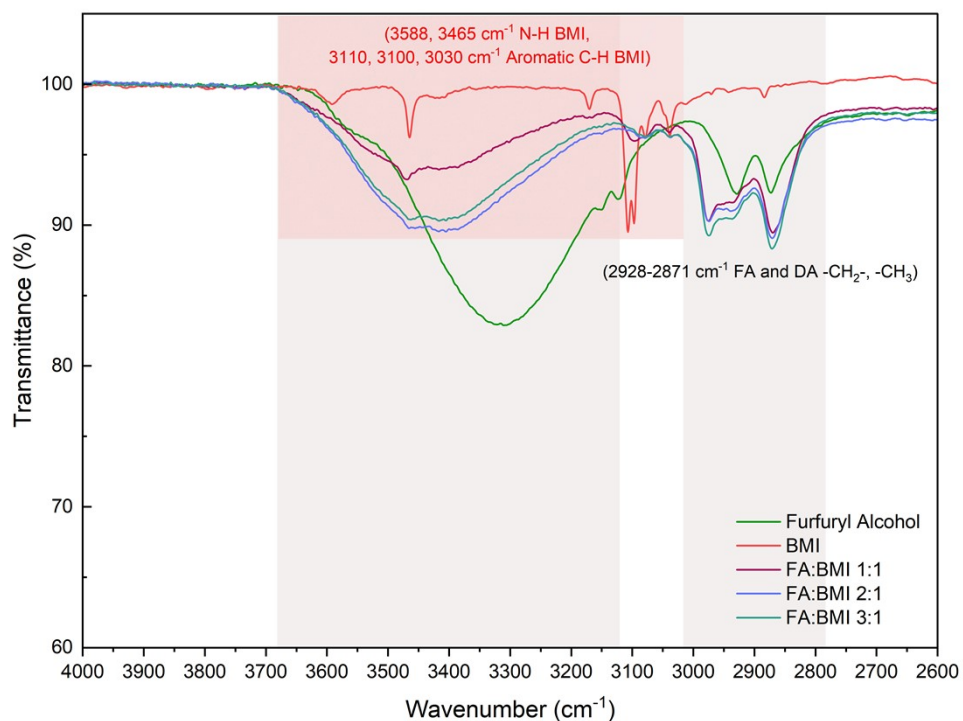


**Figure S5.** ATR-IR spectrum of optimisation studies for the model reaction with different ratios (2600-4000  $\text{cm}^{-1}$ ).

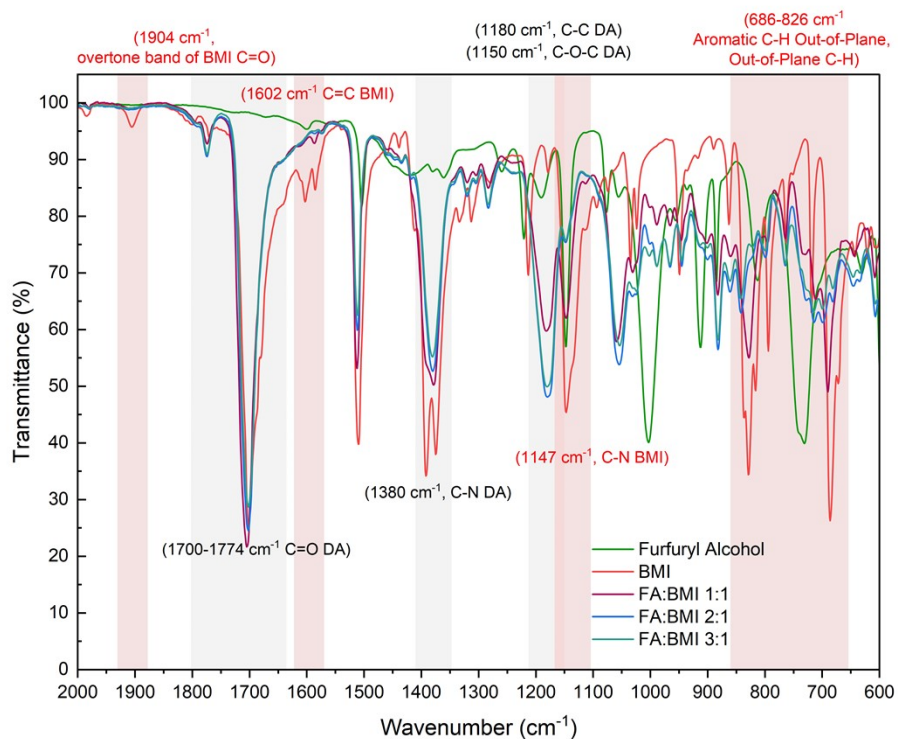


**Figure S6.** ATR-IR spectrum of optimisation studies for the model reaction with different ratios (600-2000  $\text{cm}^{-1}$ ).

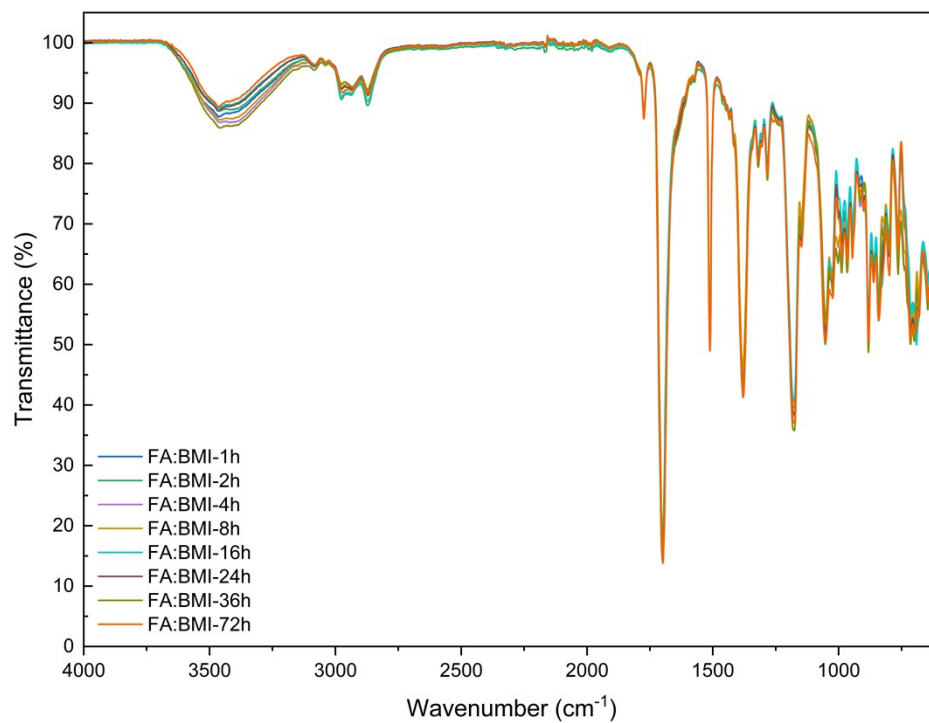


**Figure S7.** ATR-IR spectrum of optimisation studies for model reaction with different reaction times.

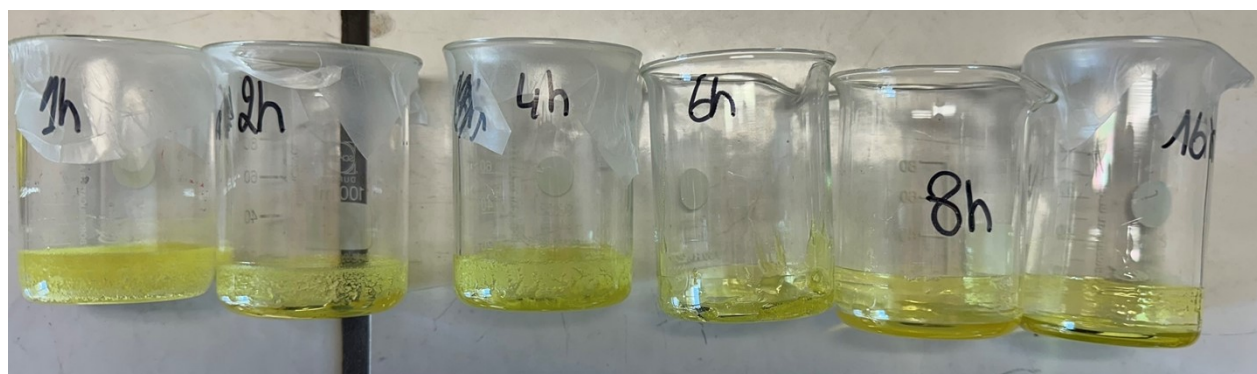


**Figure S8.** Visualisation of model reaction products at different reaction times.

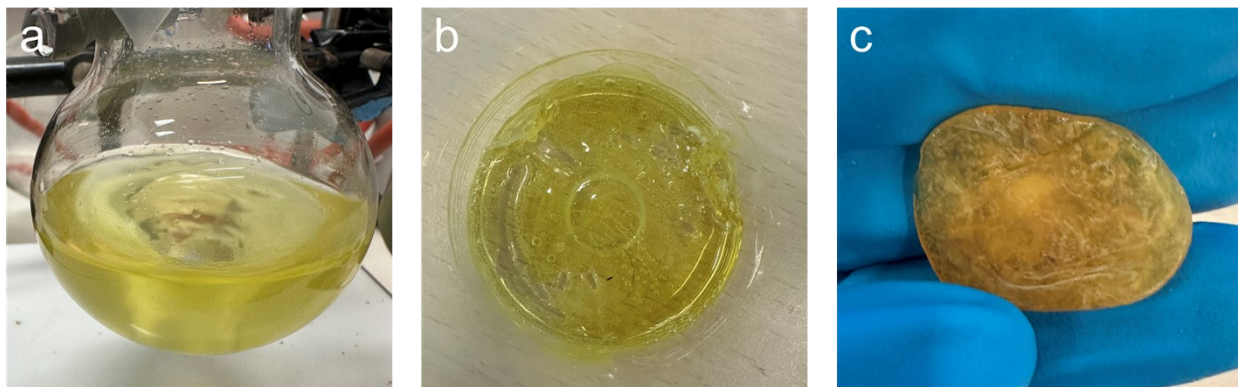


**Figure S9.** a) The reaction of 3 days when bismaleimide is fully soluble and mixed, b) the product after 2 weeks of drying, and c) after extended drying and rheological testing.

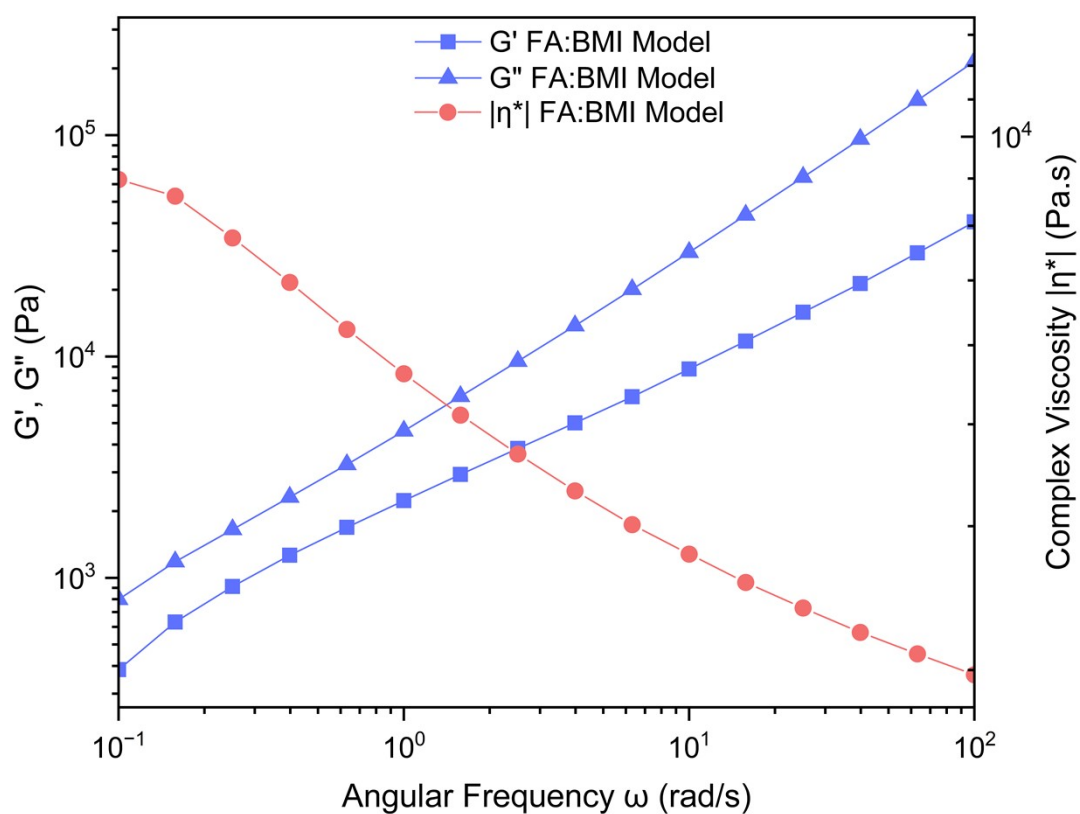


**Figure S10.** Frequency sweep tests of FA:BMI model reaction product at frequencies,  $f = 15.9$ – $0.016$  Hz ( $\omega = 100$ – $0.1$  rad  $s^{-1}$ ), and the constant strain of 1%. Experimental temperature: 25 °C

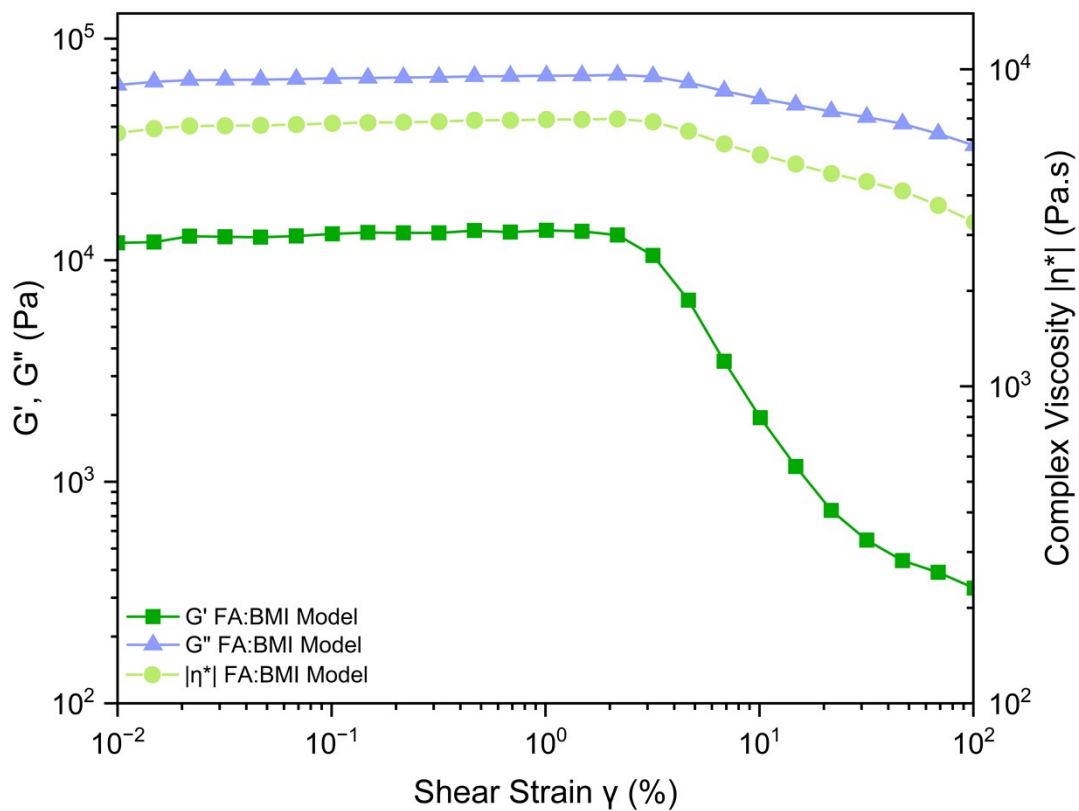


**Figure S11.** Amplitude sweep tests of FA:BMI model reaction product at strain 0.01-100% and constant frequency of 1.6 Hz, experimental temperature 25 °C.

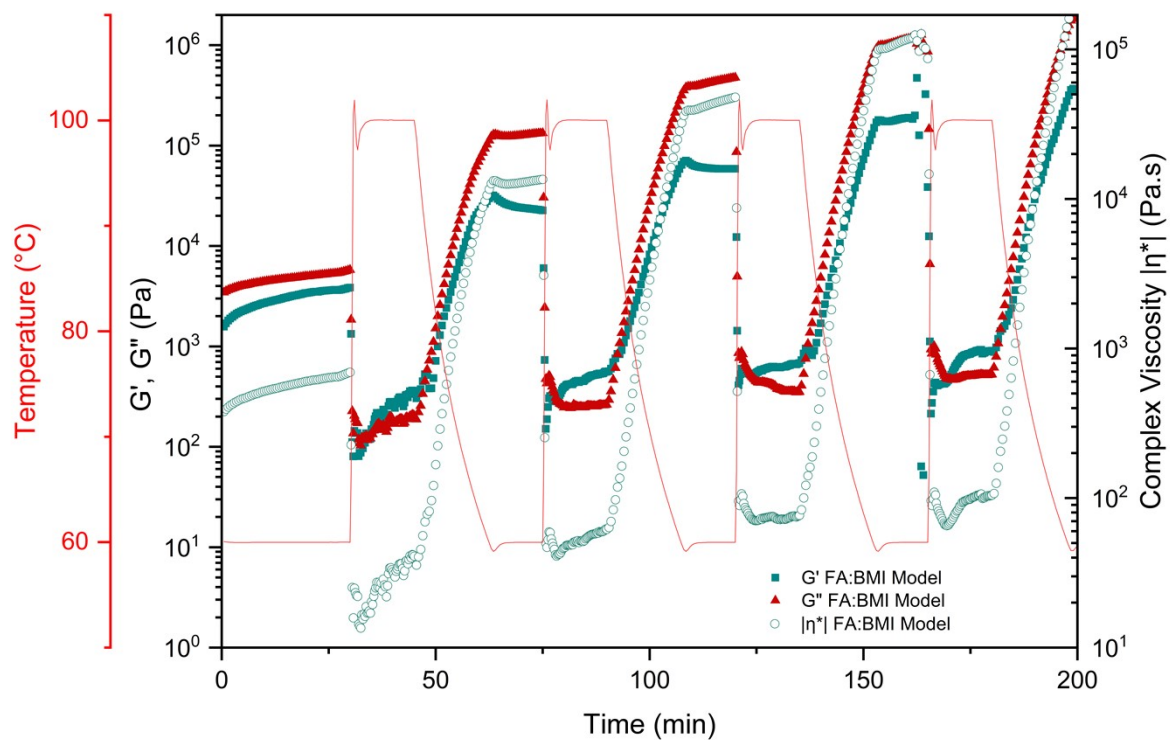


**Figure S12.** Time sweep tests of FA:BMI model reaction product at a strain of 1 % and constant frequency of 1.6 Hz with temperature varying between 60 and 100 °C.

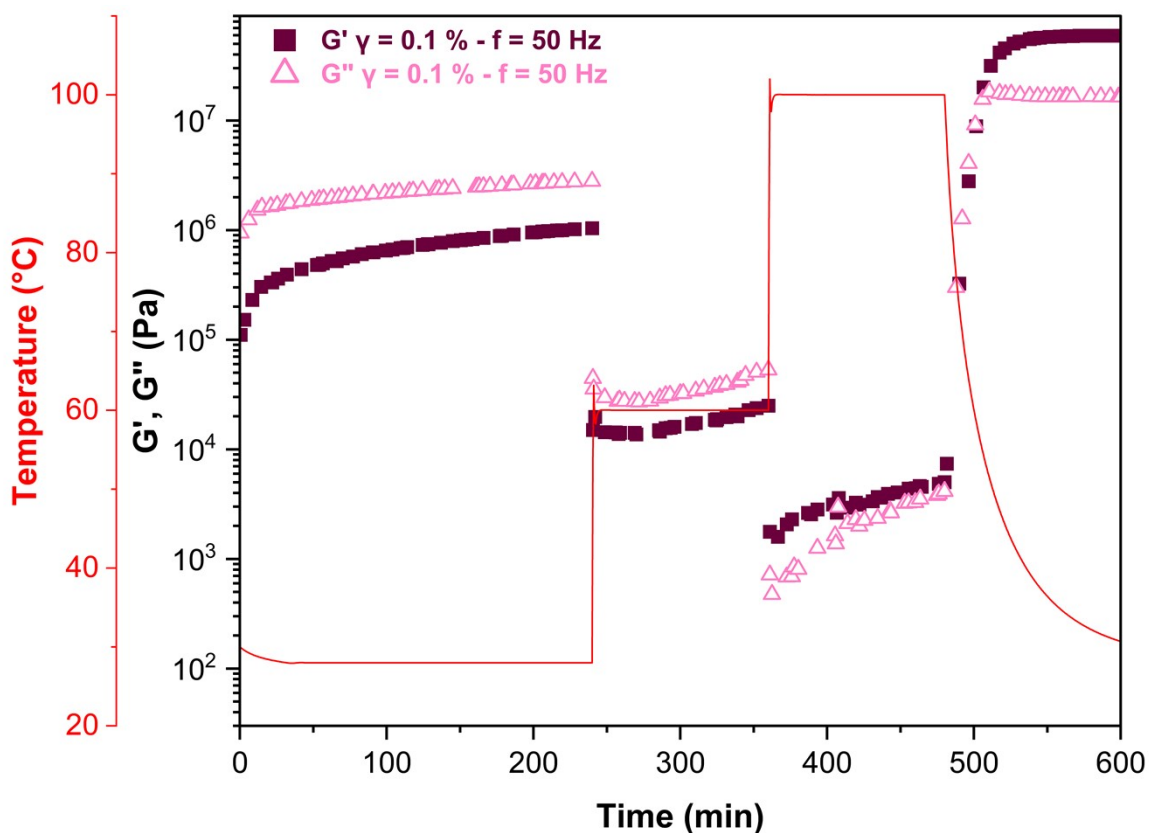


**Figure S13.** Time-resolved temperature-modulated SAOS measurements showing the evolution of storage ( $G'$ ) and loss ( $G''$ ) moduli under cyclic thermal conditions. Measurements were performed at  $\gamma = 0.1\%$  and  $f = 50$  Hz. The red line indicates the applied temperature profile.

**Table S3.** Storage modulus before and after the high-temperature segment.

Condition	$G'_{25^\circ\text{C}}$ Pa	$G'_{100^\circ\text{C}}$ Pa
$\gamma = 0.1\%$ - $f = 1$ Hz	$1.73 \times 10^5$	$9.82 \times 10^6$
$\gamma = 0.1\%$ - $f = 50$ Hz	$4.72 \times 10^5$	$5.59 \times 10^{11}$
$\gamma = 20\%$ - $f = 1$ Hz	$1.18 \times 10^4$	$6.27 \times 10^{11}$
$\gamma = 1\%$ - $f = 10$ Hz	$5.03 \times 10^4$	$1.86 \times 10^5$

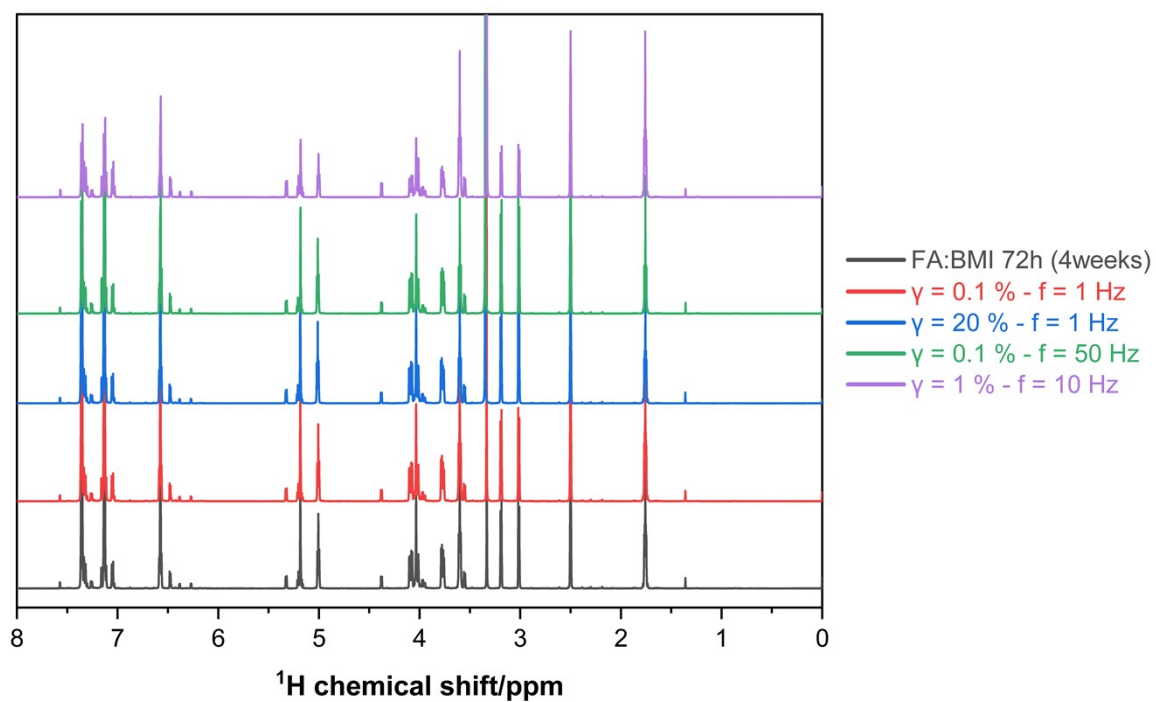


**Figure S14.** <sup>1</sup>H NMR spectra of FA:BMI model after rheological tests under different oscillatory conditions (DMSO-d<sub>6</sub>, 25 °C).

**Table S4.** <sup>1</sup>H NMR features for FA:BMI DA system.

$\delta$ (ppm)	Multiplicity <sup>1</sup>	Assignment	Observed in samples <sup>2</sup>	Comment
7.35–7.10	Aromatic protons of BMI (phenyl)	Yes	Intensity varies with DA conversion; clean multiplets.	7.35–7.10
6.40–6.20	Furan H-3 / H-4 (unreacted FA or retro-DA furan)	Yes, variable	Weakens in samples with higher DA conversion; strengthens in high- $\omega$ conditions (favouring retro-DA).	6.40–6.20
5.50–5.30	Allylic/vinyllic FA-related protons	Present but low	Sensitive to $\gamma$ ; slight shifts across conditions.	5.50–5.30
4.90–4.45	FA –CH <sub>2</sub> –O– (primary alcohol methylene)	Yes	Shifts based on DA equilibrium; diagnostic of free FA fraction.	4.90–4.45
4.40–3.70	DA bridgehead protons (endo/exo adducts)	Clear in all	Strongest DA-specific region; relative intensities reflect $\gamma$ – $\omega$ conditions.	4.40–3.70
3.70–3.20	DA bridge methylenes (–CH <sub>2</sub> –CH–in adduct)	Yes	Becomes more resolved at certain $\gamma$ – $\omega$ ; sensitive to retro-DA.	3.70–3.20
3.20–2.70	CH adjacent to imide carbonyls (BMI fragment)	All	Overlaps partly with DMSO signal (2.50 ppm).	3.20–2.70
2.50	DMSO-d <sub>6</sub>	All	Internal reference.	2.50
2.20–1.20	Backbone aliphatic protons from partial decomposition, FA side chains	Weak	Minor differences between mechanical frequencies ( $\omega$ ) are likely due to heating/local dynamics.	2.20–1.20

<sup>1</sup> *br s* = broad singlet; *br m* = broad multiplet. Given the strong broadening and overlap, these are descriptive only and do not represent discrete spin systems.

**Table S5.** Endo/exo signal intensities of FA:BMI after rheological testing (THF-corrected, normalised to 4H one benzene- aromatic reference)

Condition	Endo-1	Endo-2 (THF corrected)	Endo total	Exo-1	Exo-2	Exo total	Endo %	Exo %
FA:BMI 72h (unpurified)	2.02	1.22	3.02	0.72	0.72	1.44	67.7	32.3
FA:BMI (4 weeks)	1.90	0.54	2.44	1.32	1.29	2.61	48.3	51.7
$\gamma = 0.1\%$ - $f = 1$ Hz	1.92	0.31	2.23	1.62	1.58	3.20	41.1	58.9
$\gamma = 0.1\%$ - $f = 50$ Hz	1.94	0.32	2.26	1.58	1.55	3.13	41.9	58.1
$\gamma = 20\%$ - $f = 1$ Hz	1.94	0.35	2.29	1.57	1.55	3.12	42.3	57.7
$\gamma = 1\%$ - $f = 10$ Hz	1.97	0.31	2.28	1.59	1.56	3.15	42	58

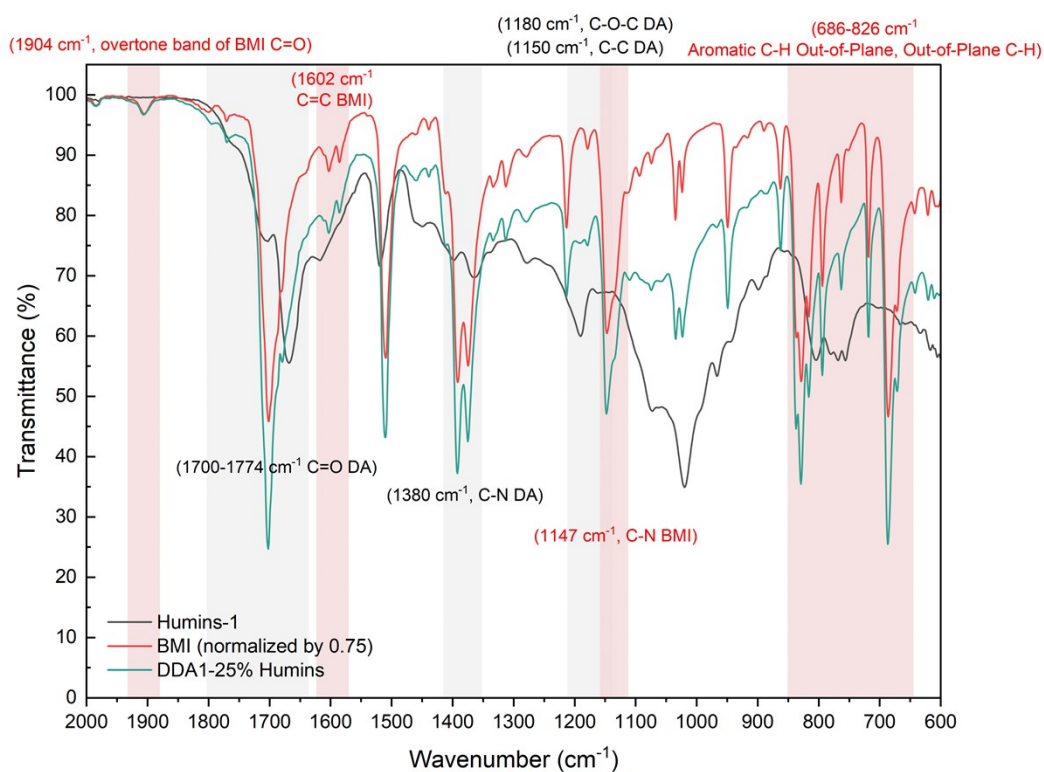


**Figure S15.** ATR-FTIR spectrum of the reaction of 75% BMI with 25% Humins1 (600-2000 cm<sup>-1</sup>).

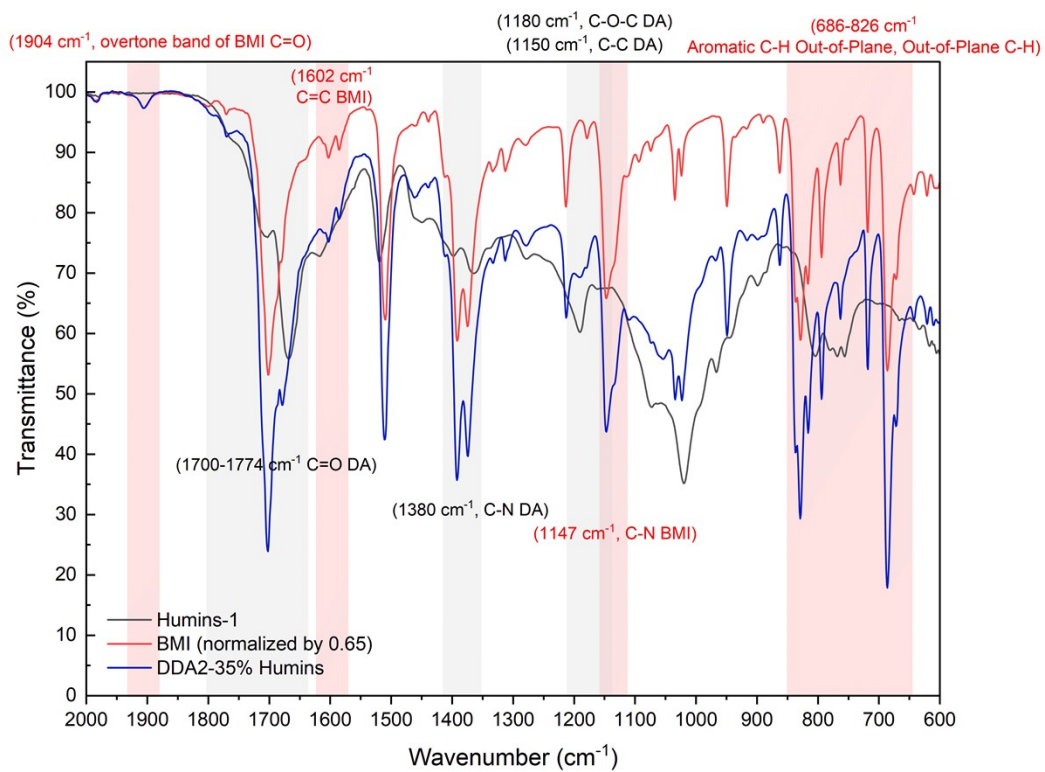


**Figure S16.** ATR-FTIR spectrum of the reaction of 65% BMI with 35% Humins1 (600-2000  $\text{cm}^{-1}$ ).

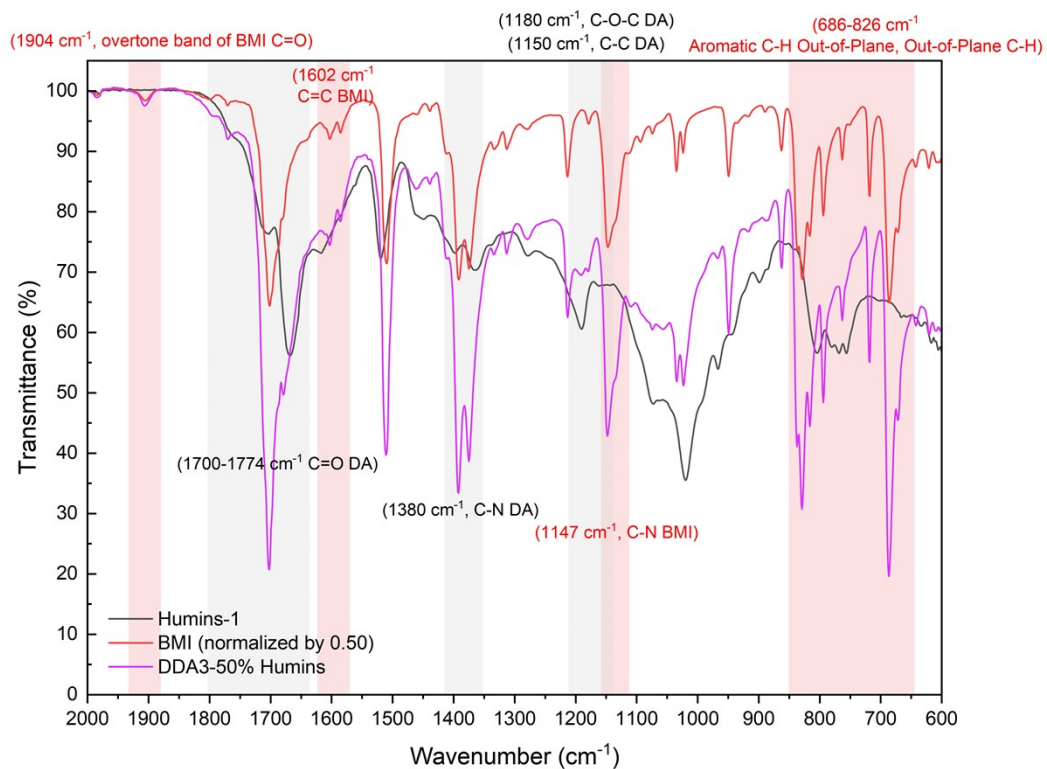


**Figure S17.** ATR-FTIR spectrum of the reaction of 50% BMI with 50% Humins1 (600-2000  $\text{cm}^{-1}$ ).

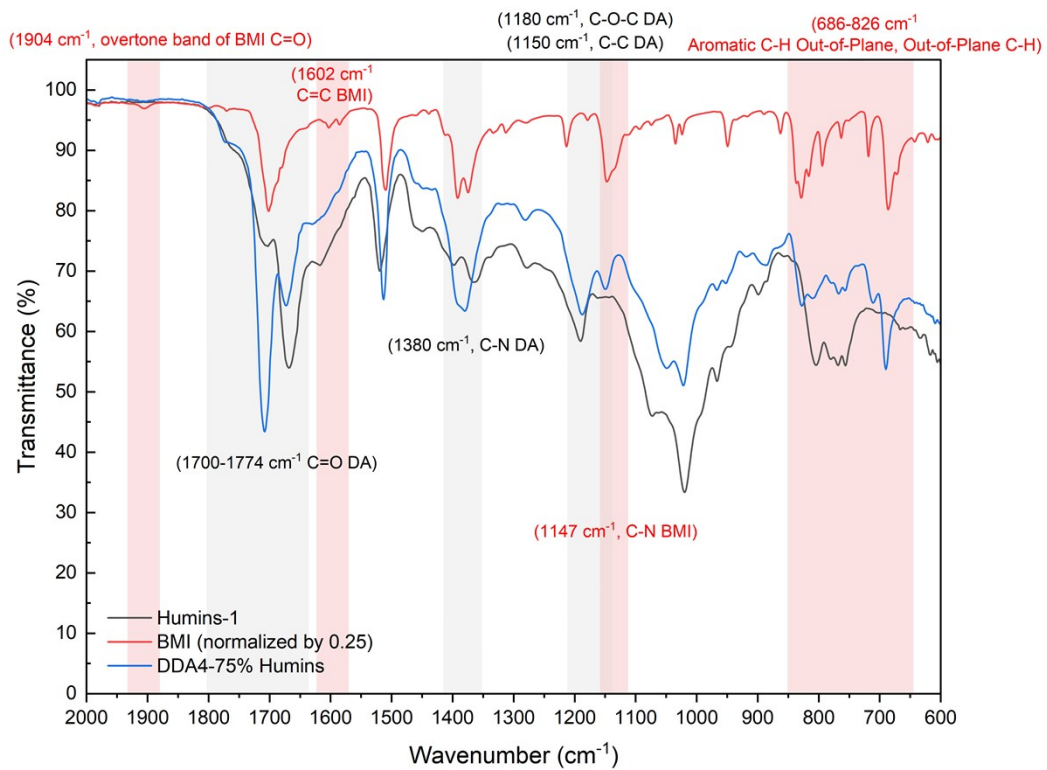


**Figure S18.** ATR-FTIR spectrum of the reaction of 25% BMI with 75% Humins1 (600-2000  $\text{cm}^{-1}$ ).

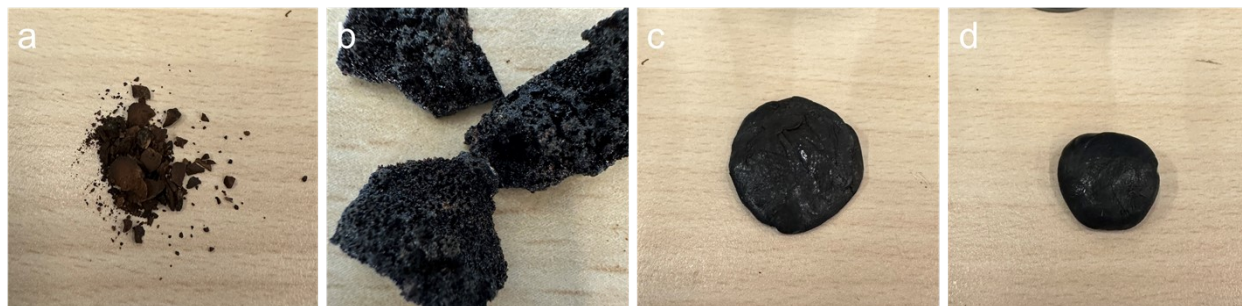


**Figure S19.** The reactions were carried out in different proportions, namely 25%, 35%, 50%, and 75% humins, respectively.

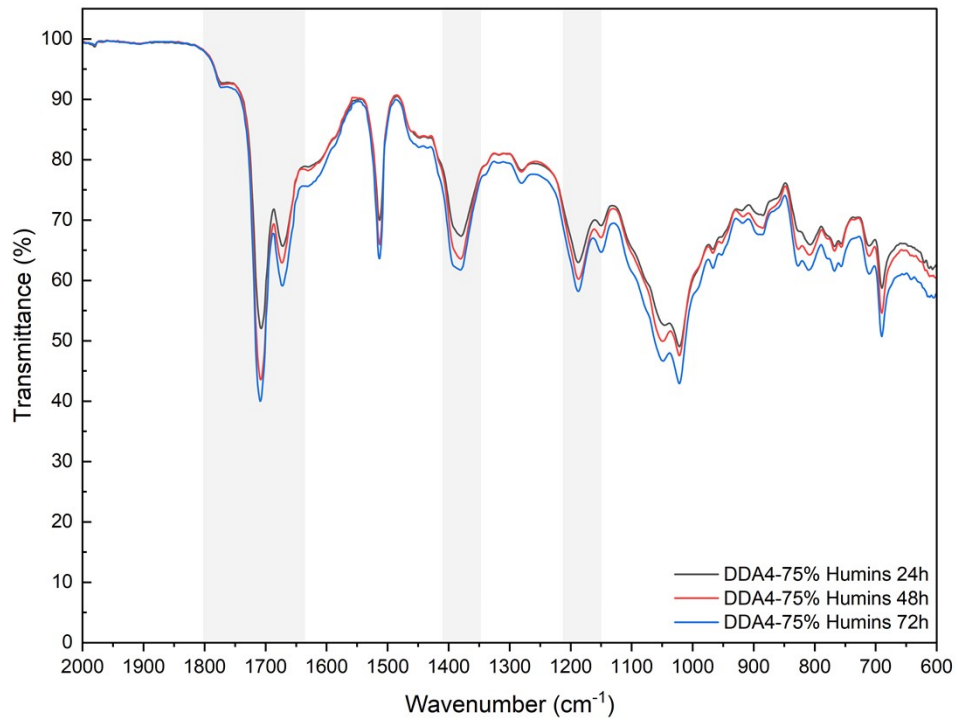


**Figure S20.** ATR-IR spectra of optimisation studies for the Diels-Alder reaction between Humins1 and BMI with different reaction times.

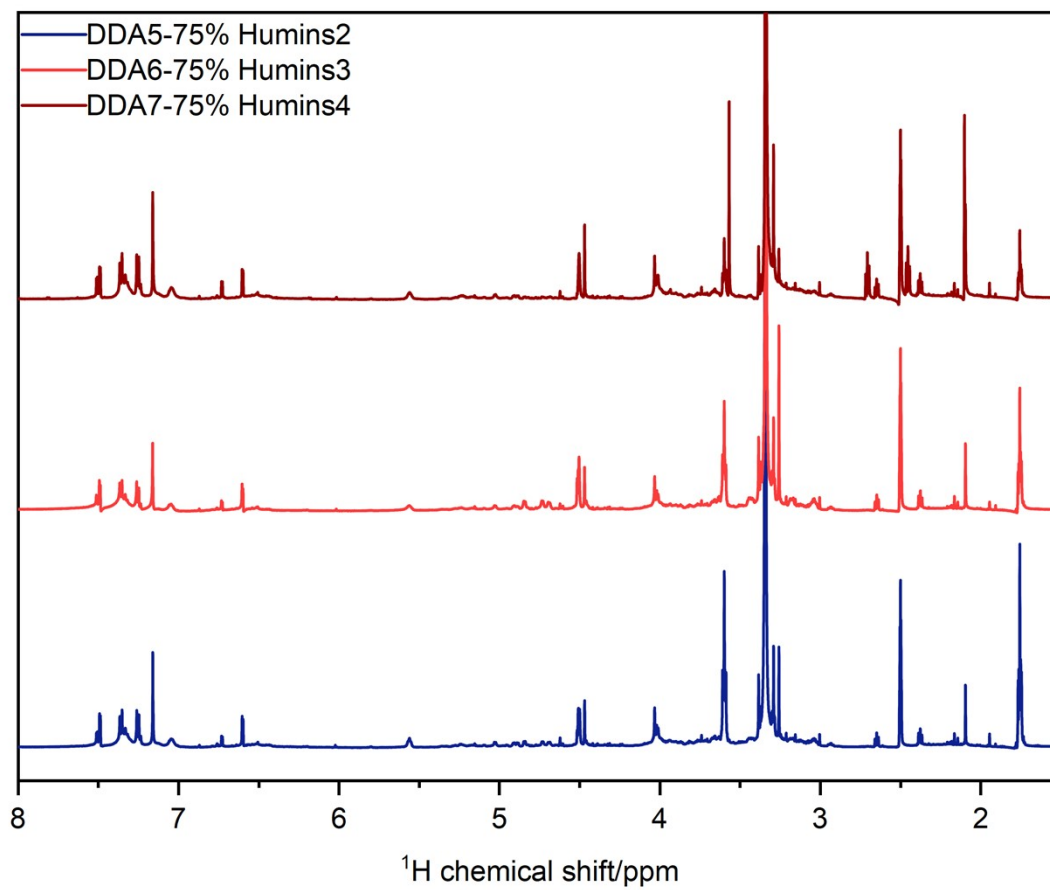


**Figure S21.** <sup>1</sup>H NMR spectra of other Diels-Alder adducts with different humins.

**Table S6.** <sup>1</sup>H NMR data for Diels–Alder-modified humins (Humins1-DDA4, Humins2-DDA5, Humins3-DDA6, Humins4-DDA7) (600 MHz, DMSO-d<sub>6</sub>, 25 °C).

$\delta$ (ppm)	Multiplicity <sup>1</sup>	Assignment	Observed in samples <sup>2</sup>	Comment
12.5–10.0	br s	COOH / strongly H-bonded phenolic OH (humins)	All DA samples	Similar to parent humins; minor changes in intensity only.
9.8–8.5	br s / br m	Aldehydic/formyl protons	All DA samples (weak)	Residual oxidised end groups; often low intensity.
8.5–7.5	br m	Aromatic/oxidised furanic protons (humins)	All DA samples	Background humins envelope retained.
7.5–7.0	br m	Aromatic protons of BMI phenyl rings + overlapping humins aromatics	All DA samples	New contribution from BMI vs. parent humins; appears as a slightly more structured shoulder.
7.0–6.0	br m	Remaining furanic/aromatic protons	All DA samples	Broad hump, inherited mainly from humins.
6.2–5.8	br m	Residual vinylic / conjugated C=C–H (if present)	Some DA samples (weak)	Often, it is strongly reduced compared to the parent if the double bond is consumed by DA.
5.5–4.8	br m	O–CH / acetal-like protons (humins matrix)	All DA samples	Overlaps partially with the high-field side of the DA bridge signals.
4.8–4.0	br m	Bridgehead/bridge methine protons of DA adduct (furan–BMI)	All DA samples (diagnostic)	New broad envelope vs. parent humins, consistent with DA ring formation.
4.0–3.2	br m	Bridge methylene (–CH <sub>2</sub> –) of DA adduct + CH <sub>2</sub> –O / CH–O in humins	All DA samples	DA-related signals superimposed on humins O–CH <sub>2</sub> region; appears as an intensity increase.
3.2–2.5	br m	Aliphatic CH/CH <sub>2</sub> adjacent to imide and carbonyl groups (BMI fragment)	All DA samples	Often broadened; may partially overlap with DMSO-d <sub>6</sub> residual (~2.50 ppm).

2.5–1.8	br m	Aliphatic CH / CH <sub>2</sub> from humins backbone and DA linkages	All DA samples	Similar to humins, slightly more intense due to the addition of DA aliphatic carbons.
1.8–1.0	br m	Saturated CH <sub>2</sub> /CH groups, remote from heteroatoms	All DA samples	Broad hump, no resolved pattern.
1.0–0.5	br m	Terminal CH <sub>3</sub> and other aliphatic end groups	All DA samples	Low-intensity, very broad; consistent with aliphatic chain ends and BMI-derived fragments.

Diels–Alder modification of humins with bismaleimide (BMI) preserves the broad humins background signals and introduces additional aliphatic and aromatic resonances associated with the DA adduct and the BMI fragment. As for the parent humins, broadening and overlap preclude meaningful reporting of individual integrals and coupling constants.

<sup>1</sup> br s = broad singlet; br m = broad multiplet. Given the strong broadening and overlap, these are descriptive only and do not represent discrete spin systems.

<sup>2</sup> Humins1-DDA4, Humins2-DDA5, Humins3-DDA6, and Humins4-DDA7 all show qualitatively similar features. Minor variations in relative intensities reflect differences in humins batch composition and DA conversion.

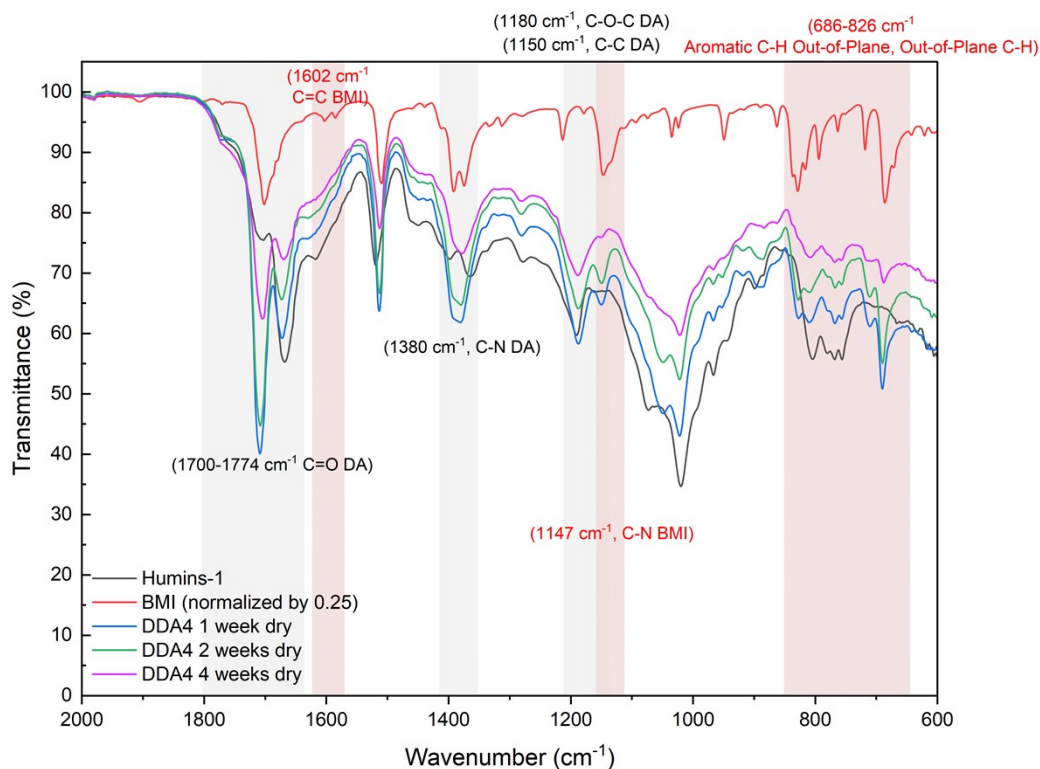


**Figure S22.** The ATR-IR spectrum of the Diels–Alder reaction product with Humins1 was analysed at specific intervals.

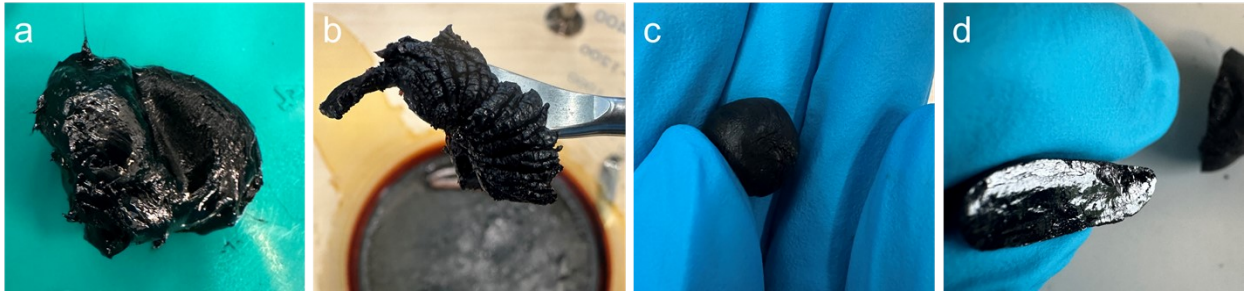


**Figure S23.** Periodic photographs of the Diels-Alder reaction product with Humins1 recorded after (a) 3 days, (b) 1 week, (c) 2 weeks, (d) 4 weeks, respectively.

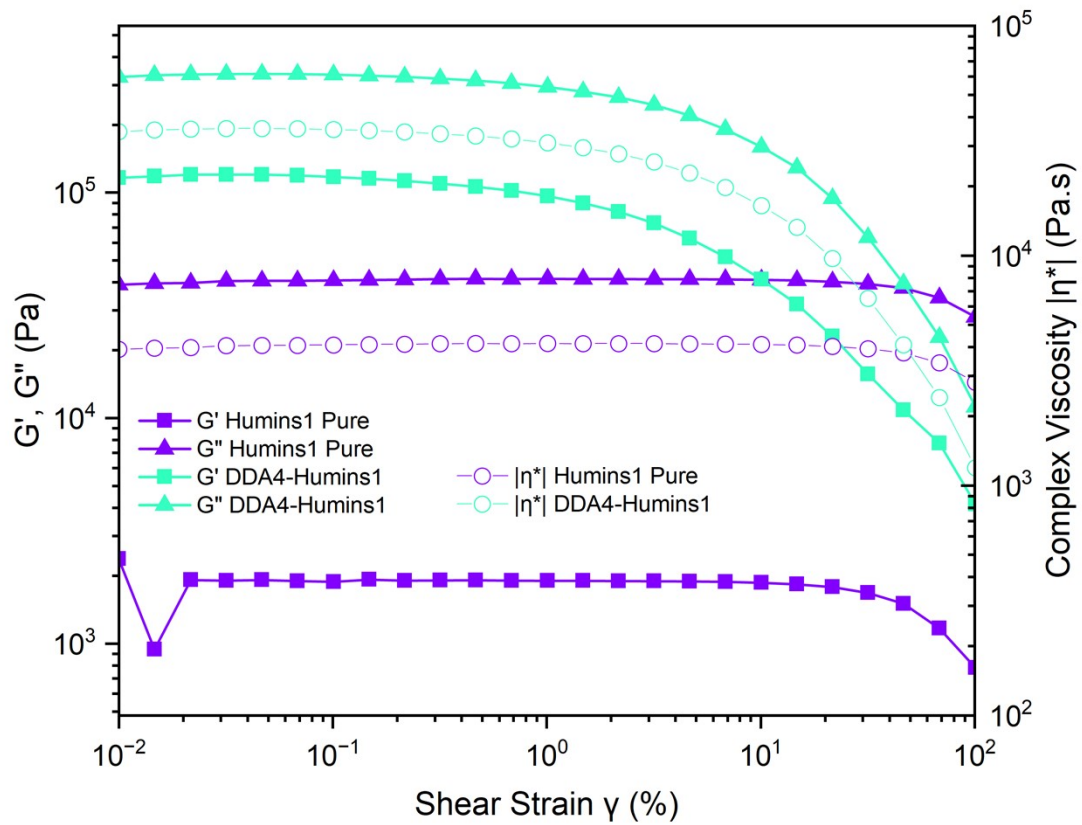


**Figure S24.** Amplitude sweep tests of neat Humins1 and 75:25 w/w Humins1:BMI Diels-Alder product at strain 0.01–100 % and constant frequency of 1.6 Hz. Experimental temperature: 25 °C.

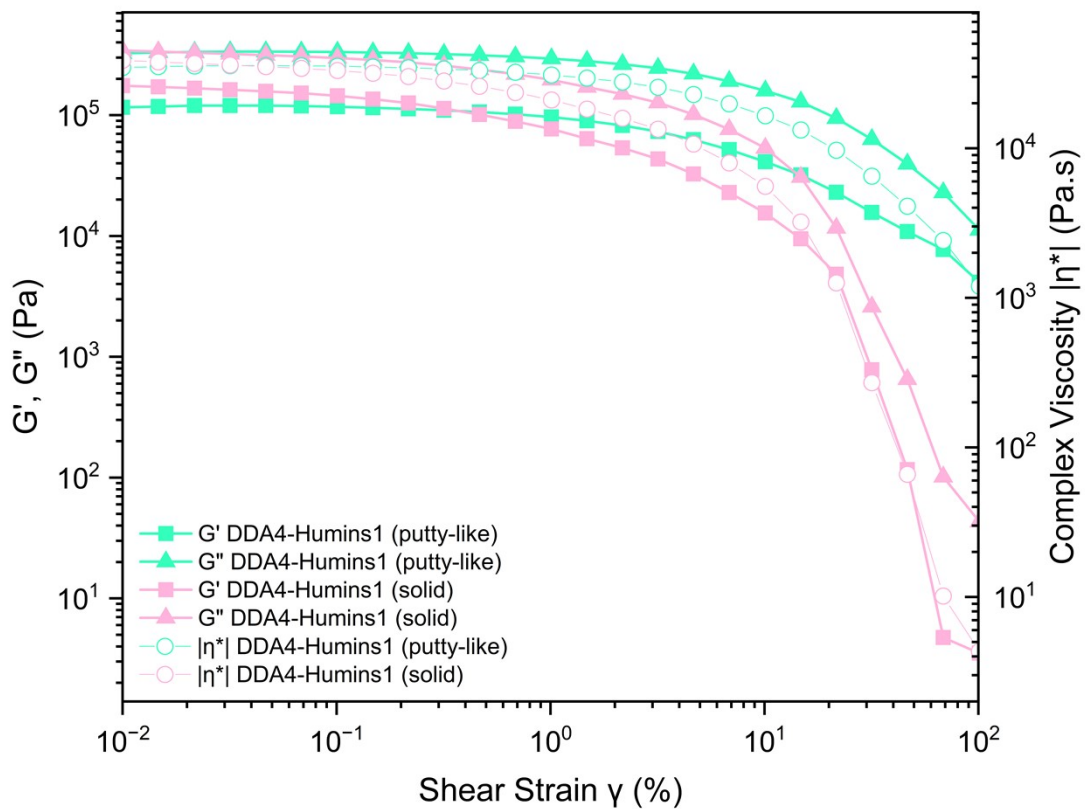


**Figure S25.** Amplitude sweep tests of DDA4-Humins1 product after 2 and 4 weeks drying at strain 0.01–100 % and constant frequency of 1.6 Hz. Experimental temperatures: 25 °C for a 2-week putty-like sample and 60 °C for a 4-week solid sample.

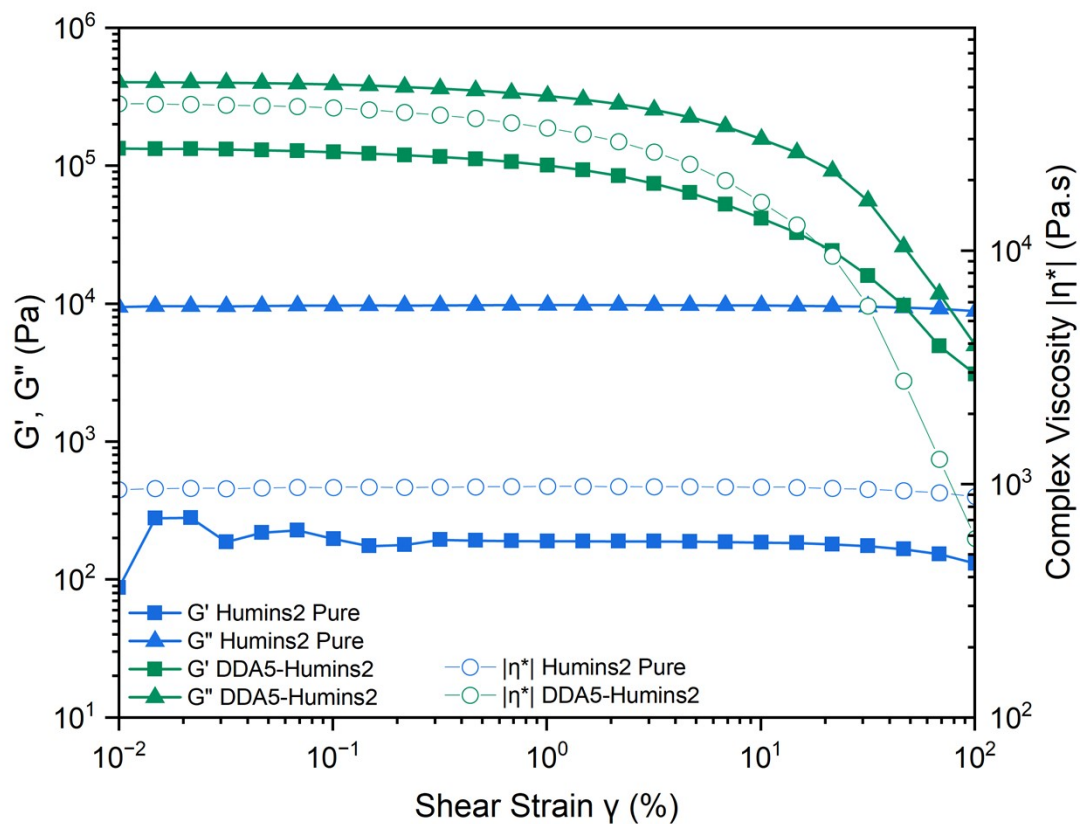


**Figure S26.** Amplitude sweep tests of neat Humins2 and 75:25 w/w Humins2:BMI Diels–Alder product at strain 0.01–100 % and constant frequency of 1.6 Hz. Experimental temperature: 25 °C.

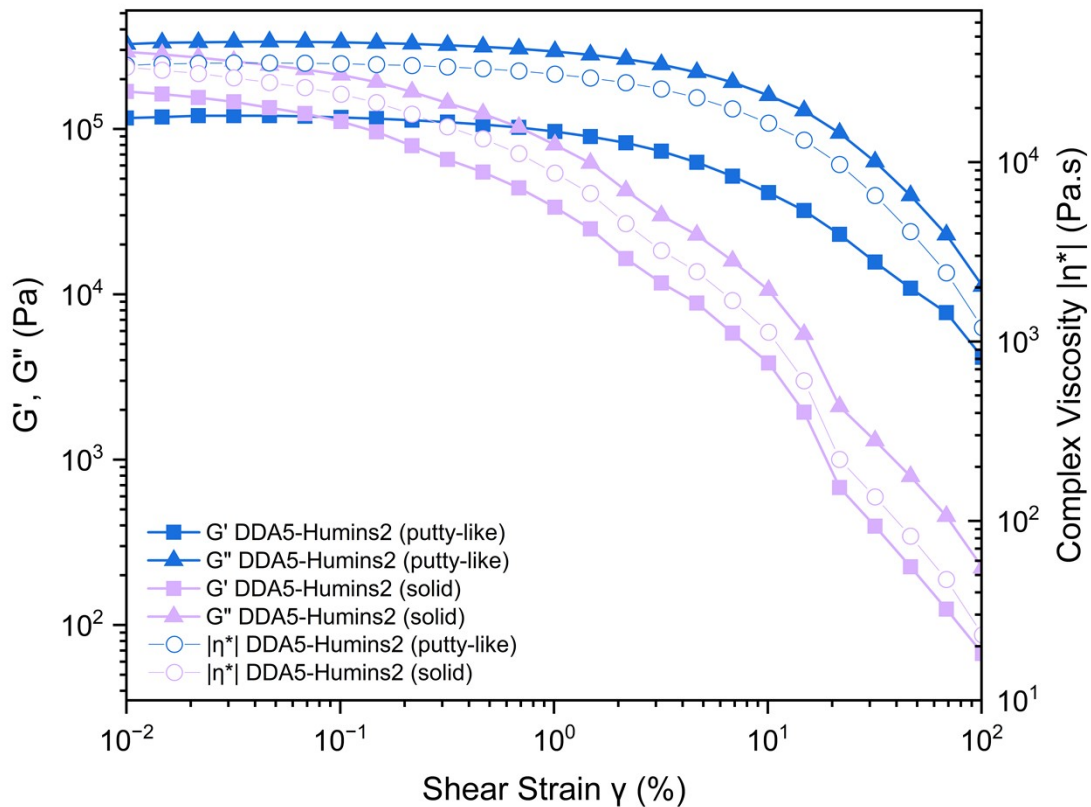


**Figure S27.** Amplitude sweep tests of DDA5-Humins2 product after 2 and 4 weeks drying at strain 0.01–100 % and constant frequency of 1.6 Hz. Experimental temperatures: 25 °C for the 2-week putty-like sample and 60 °C for the 4-week solid sample.

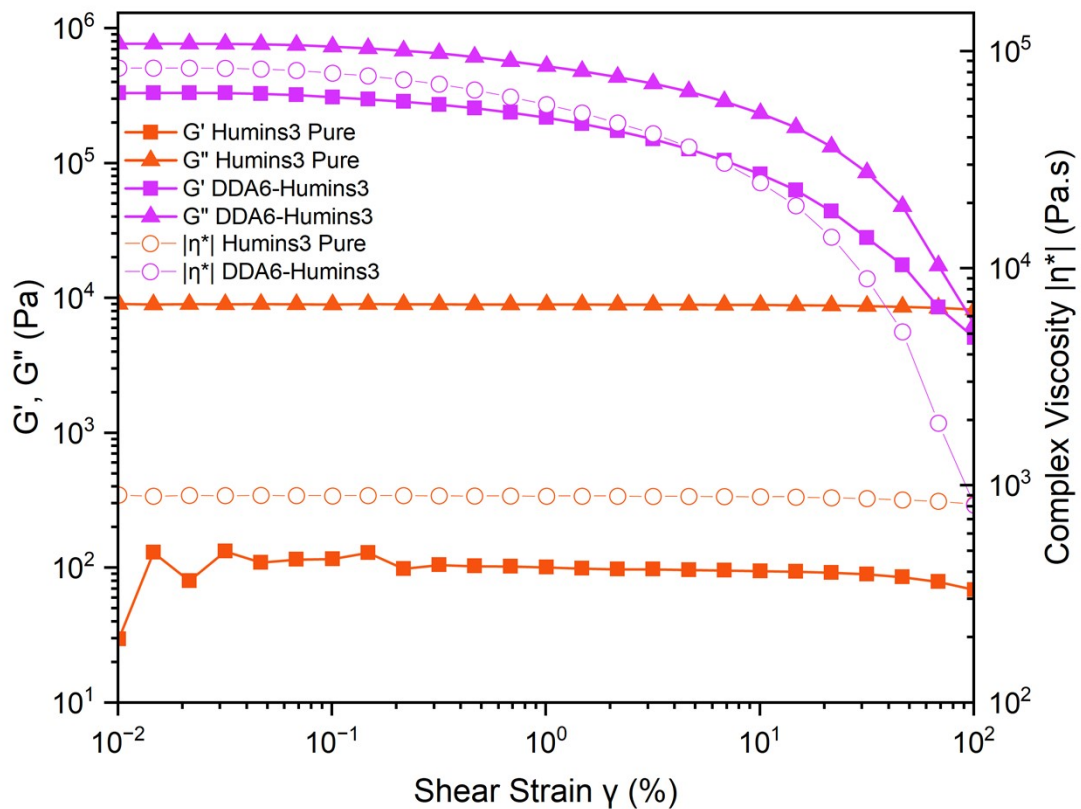


**Figure S28.** Amplitude sweep tests of neat Humins3 and 75:25 w/w Humins3:BMI Diels–Alder product at strain 0.01–100 % and constant frequency of 1.6 Hz. Experimental temperature: 25 °C.

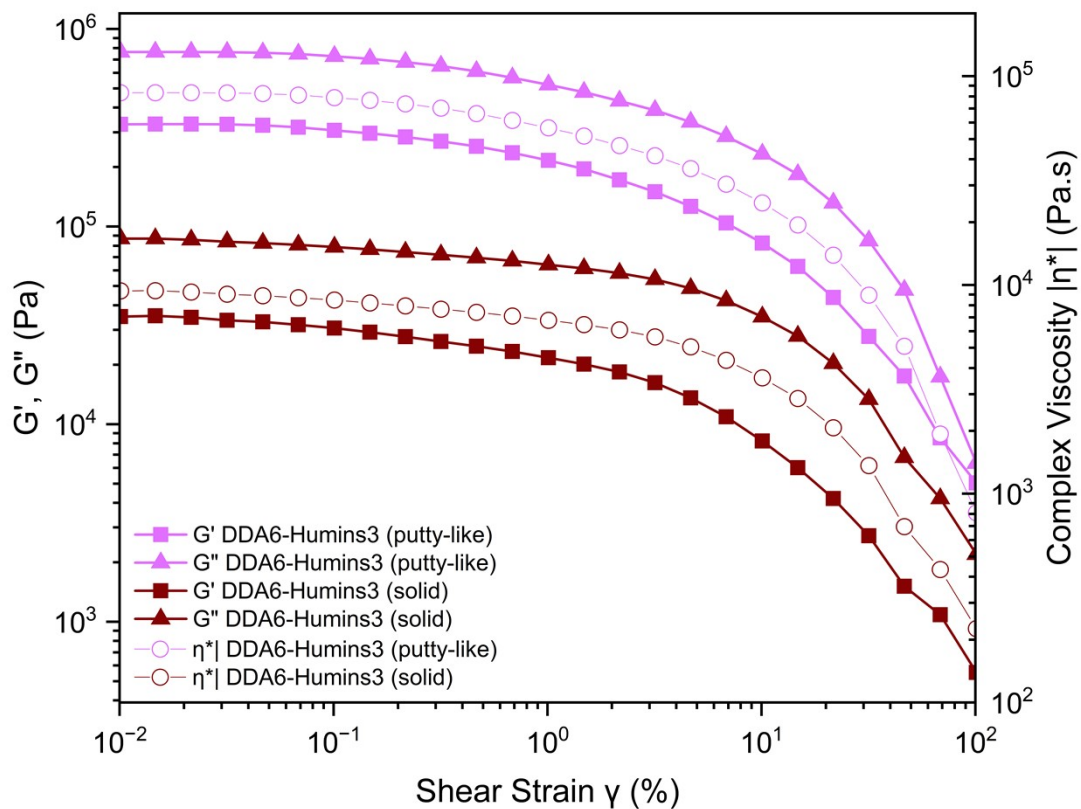


**Figure S29.** Amplitude sweep tests of DDA6-Humins3 product after 2 and 4 weeks drying at strain 0.01–100 % and constant frequency of 1.6 Hz. Experimental temperatures: 25 °C for the 2-week putty-like sample and 60 °C for the 4-week solid sample.

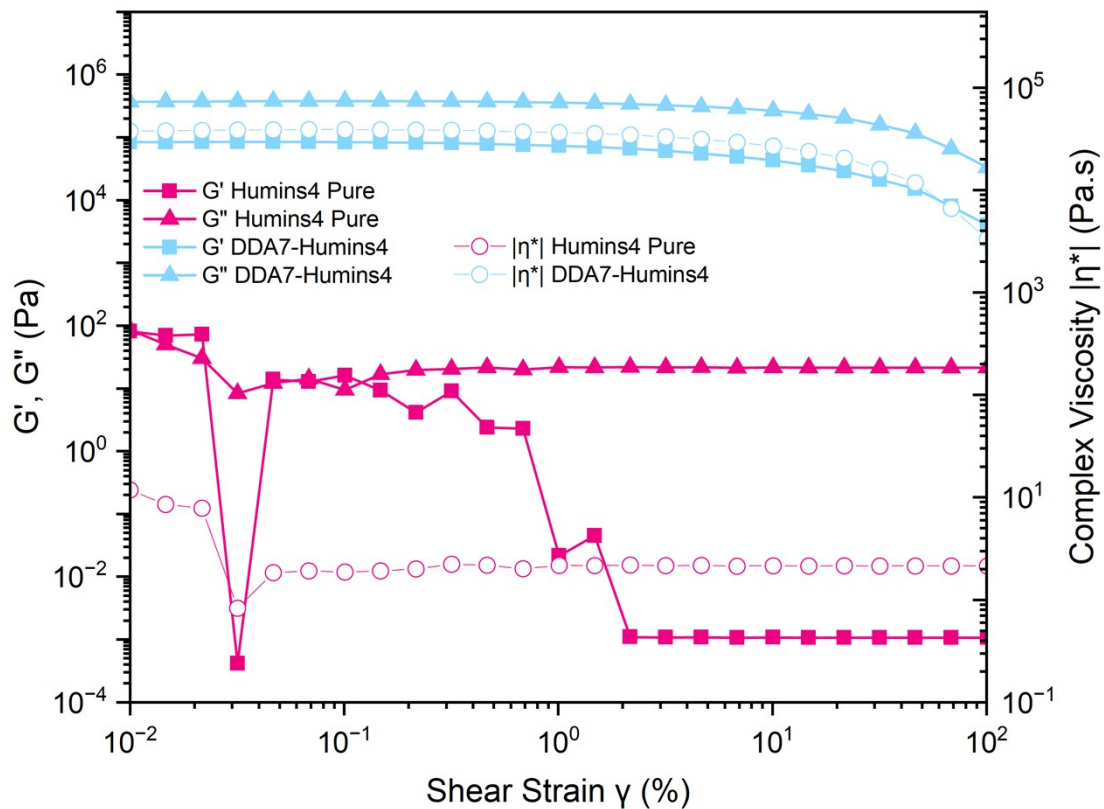


**Figure S30.** Amplitude sweep tests of neat Humins4 and 75:25 w/w Humins4:BMI Diels–Alder product at strain 0.01–100 % and constant frequency of 1.6 Hz. Experimental temperature: 25 °C.

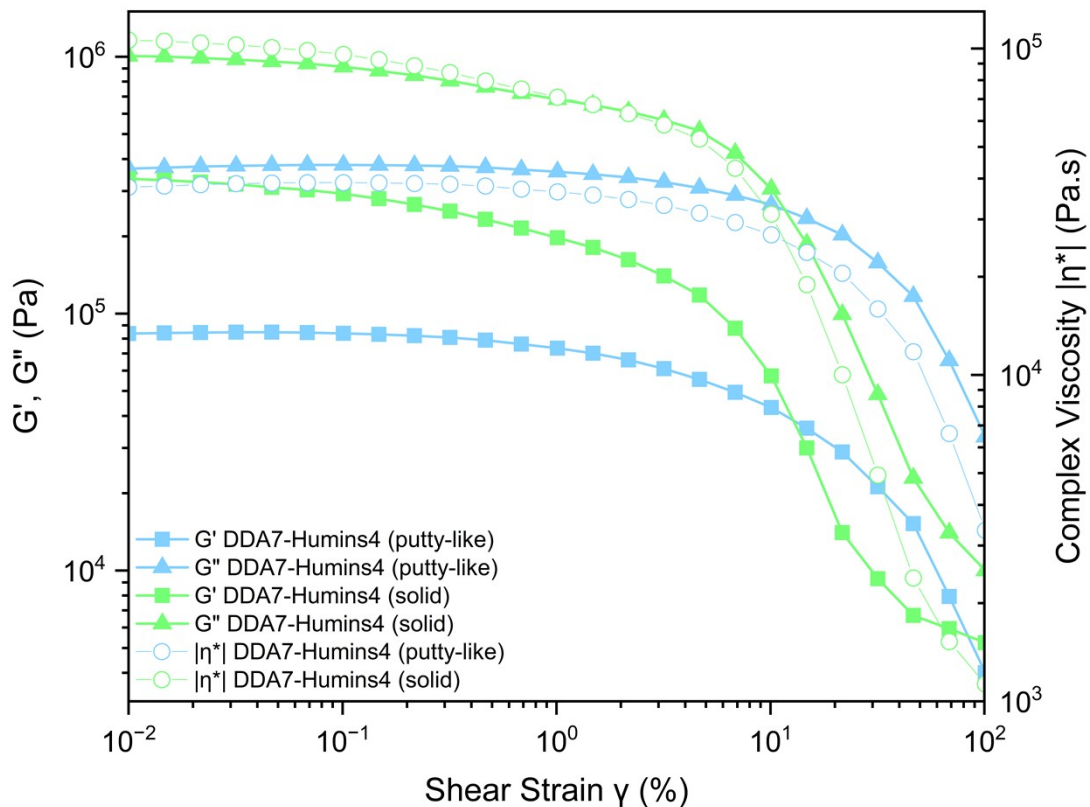


**Figure S31.** Amplitude sweep tests of DDA7-Humins4 product after 2 and 6 weeks drying at strain 0.01–100 % and constant frequency of 1.6 Hz. Experimental temperatures: 25 °C for the 2-week putty-like sample and 60 °C for the 6-week solid sample.

**Table S7.** Summary of amplitude-sweep parameters for humins and their Diels–Alder (DA)-modified counterparts, showing the increase in storage modulus ( $G'$ ), decrease in  $\tan \delta$ , extension of the linear viscoelastic region (LVR), and power-law slopes ( $m$ ) indicating strong strain-thinning at high strain.

Sample	$G'$ plateau (Pa)	$\tan \delta$ (plateau)	$\gamma_{\text{LVR}}$ (%)	$m$ ( $ \eta^* $ vs $\gamma$ )
Humins1	$2.37 \times 10^3$	39.1	0.01	-0.02
DDA4 putty-like	$1.16 \times 10^5$	3.26	0.15	-0.81
DDA4 solid	$1.75 \times 10^5$	2.90	0.01	-0.23
Humins2	$2.4 \times 10^2$	40.9	0.01	-0.02
DDA5 putty-like	$1.31 \times 10^5$	3.05	0.15	-0.81
DDA5 solid	$1.49 \times 10^5$	1.76	0.01	-0.23
Humins3	$2.0 \times 10^4$	54.9	0.01	-0.02
DDA6 putty-like	$3.29 \times 10^5$	2.32	0.10	-0.83
DDA6 solid	$3.41 \times 10^4$	2.49	0.07	-0.70
Humins4	$3.9 \times 10^4$	5000*	0.01	0.03
DDA7 putty-like	$8.45 \times 10^4$	4.43	0.47	-0.43
DDA7 solid	$3.21 \times 10^5$	3.05	0.07	-0.98

\*Abnormally high  $\tan \delta$  due to the low-modulus limit of the instrument.

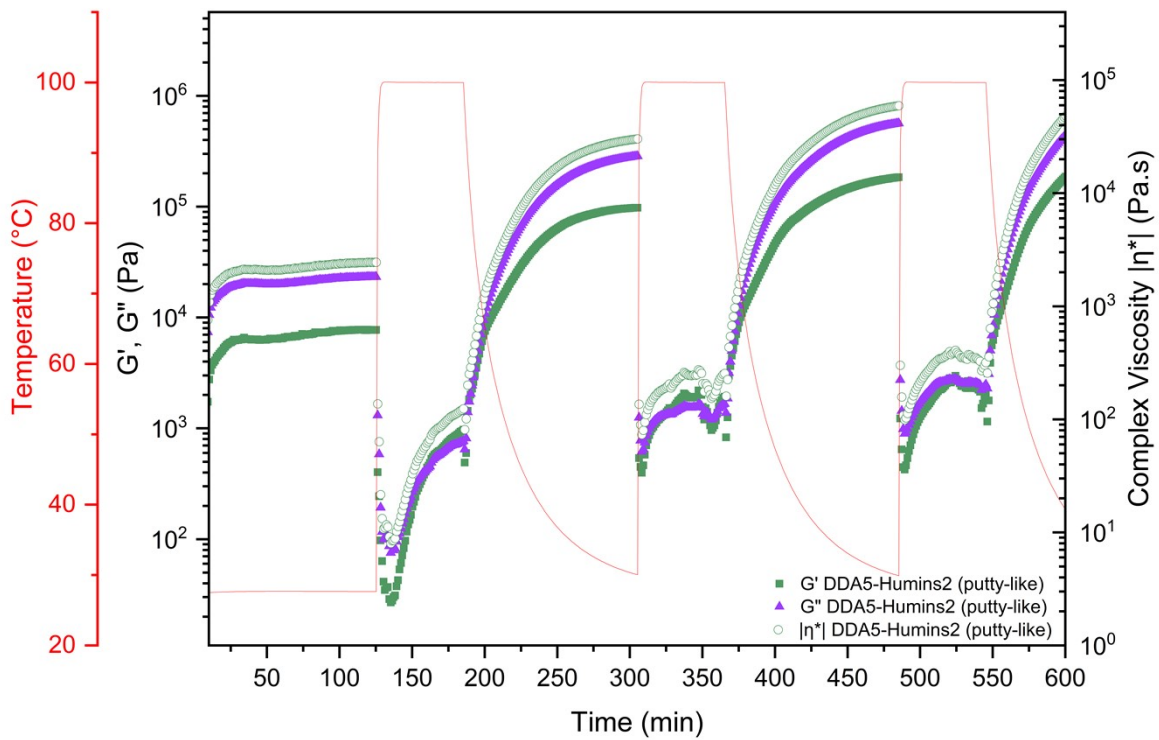


**Figure S32.** Time sweep tests of DDA5-Humins2 at a strain of 1 % and constant frequency of 1.6 Hz with temperature varying between 25 and 100 °C (putty-like sample, 2 weeks).

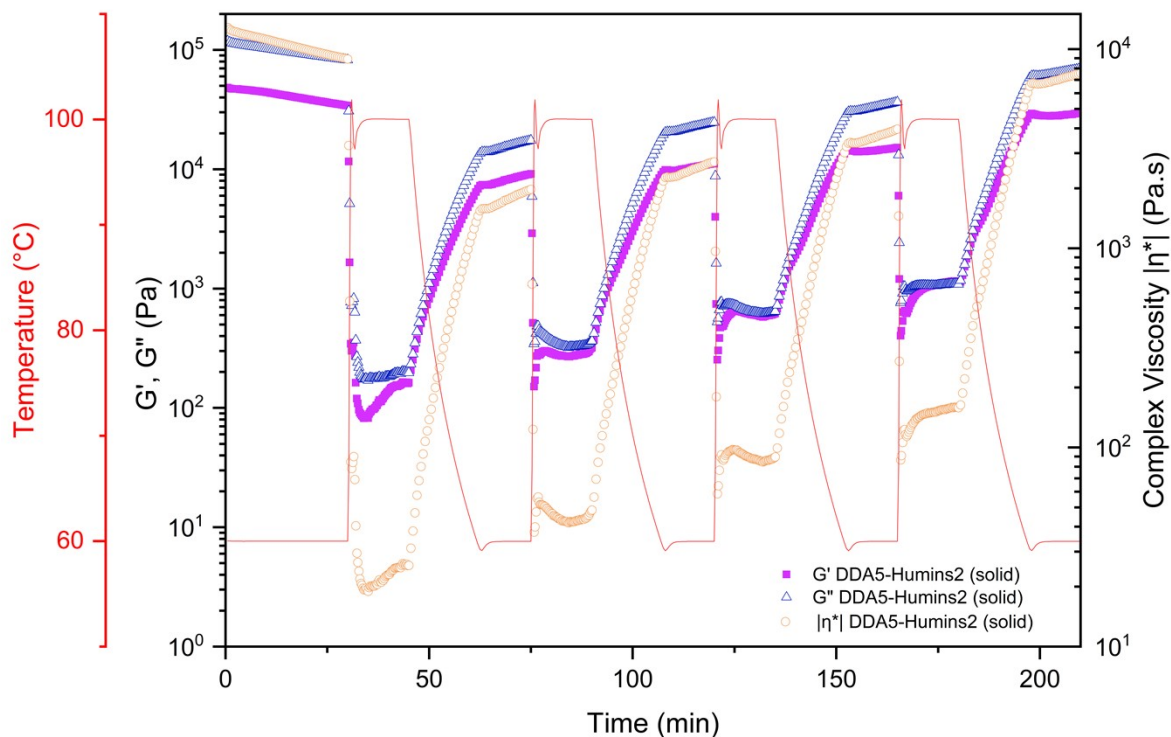


**Figure S33.** Time sweep tests of DDA5-Humins2 at a strain of 1 % and constant frequency of 1.6 Hz with temperature varying between 60 and 100 °C (solid material, 4 weeks).

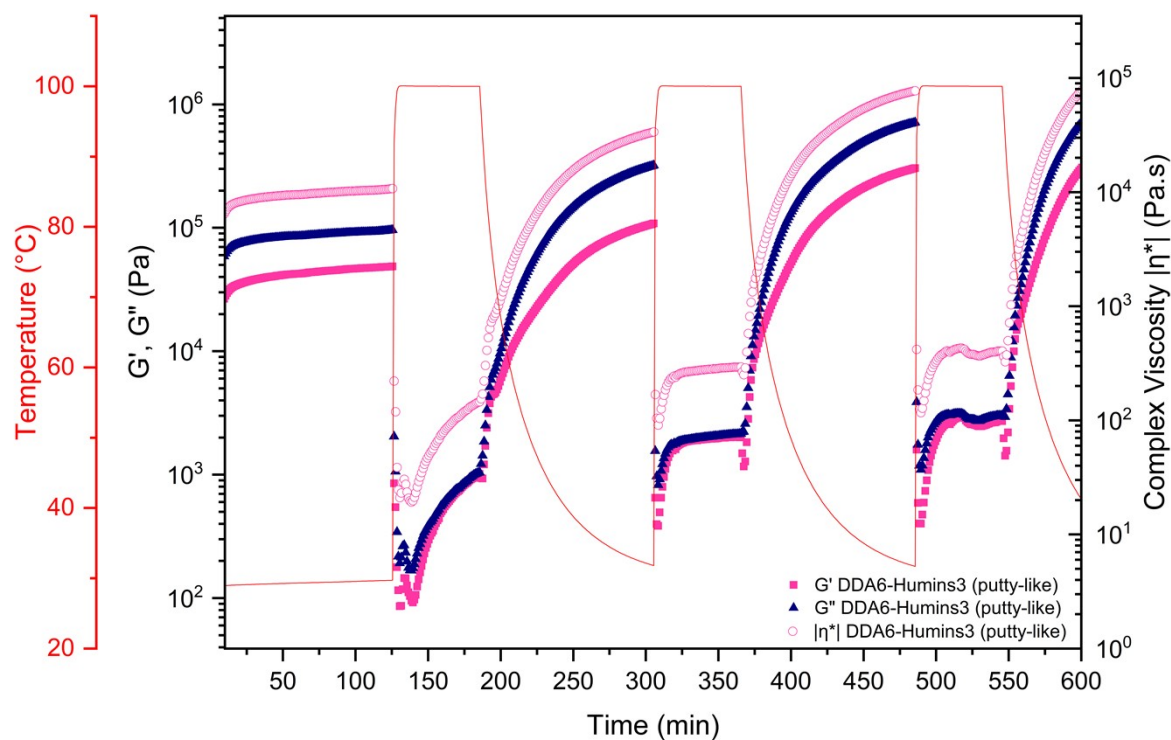


**Figure S34.** Time sweep tests of DDA6-Humins3 at a strain of 1 % and constant frequency of 1.6 Hz with temperature varying between 25 and 100 °C (putty-like material, 2 weeks).

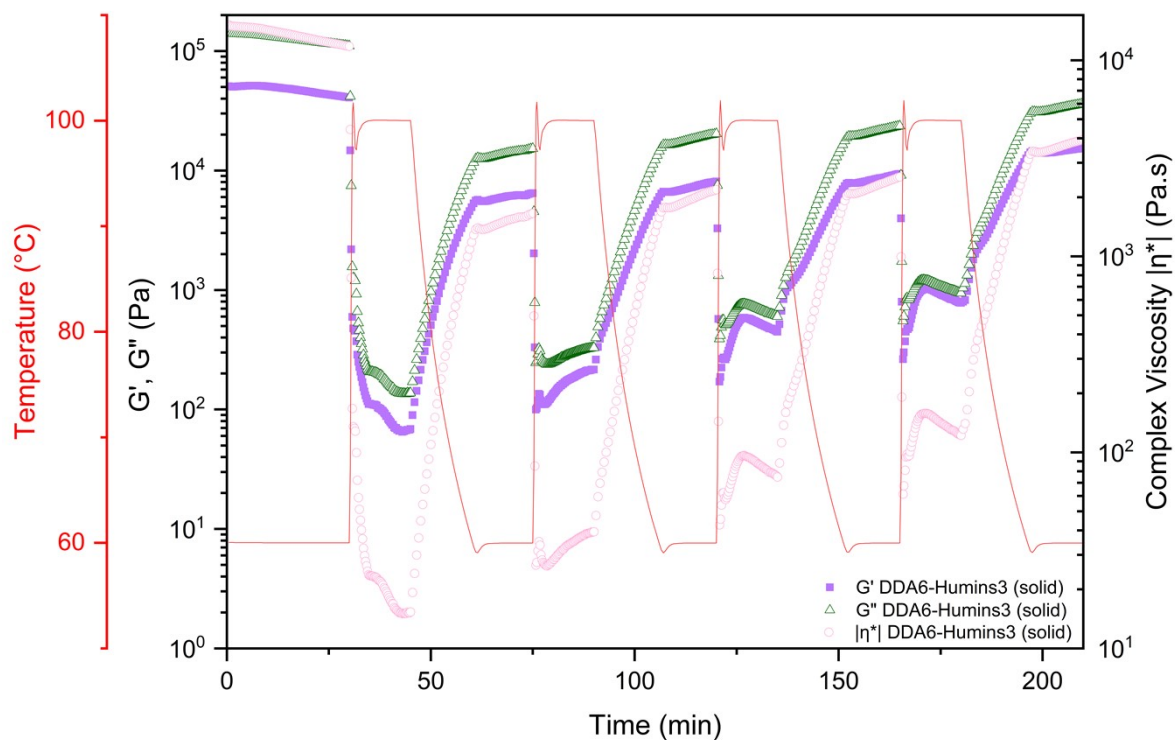


**Figure S35.** Time sweep tests of DDA6-Humins3 at a strain of 1 % and constant frequency of 1.6 Hz with temperature varying between 60 and 100 °C (solid material, 4 weeks).

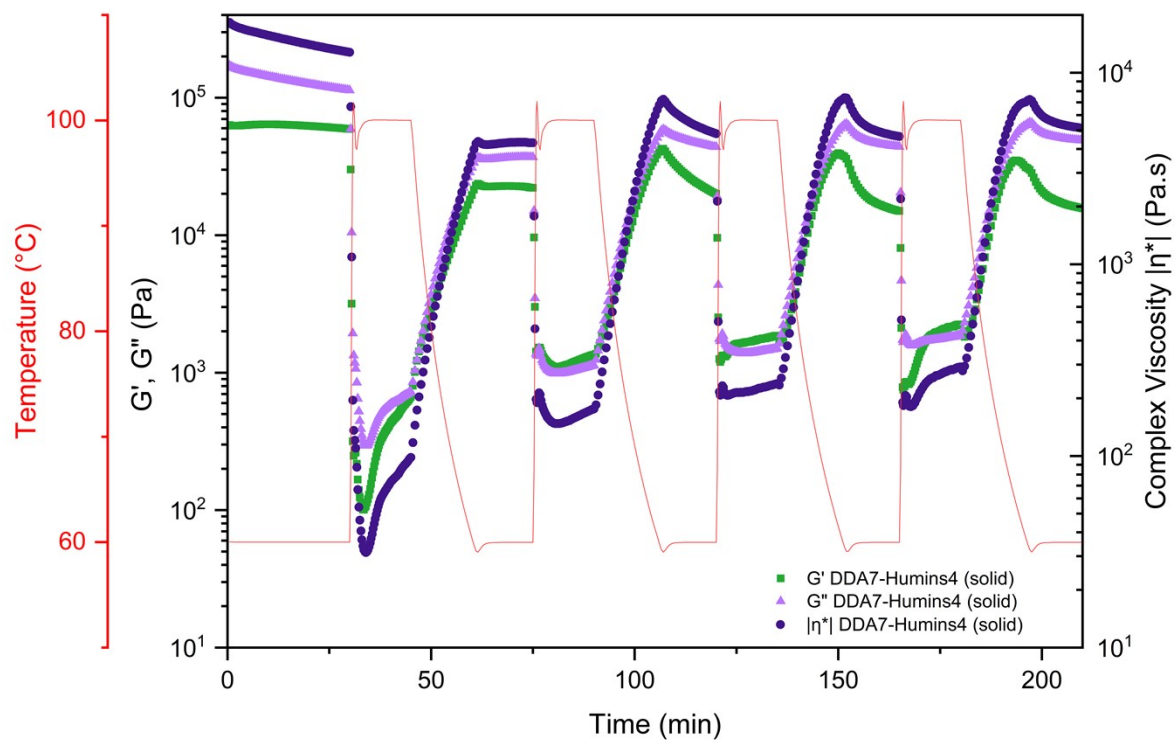


**Figure S36.** Time sweep tests of DDA7-Humins4 at a strain of 1 % and constant frequency of 1.6 Hz with temperature varying between 60 and 100 °C (solid material, 6 weeks).

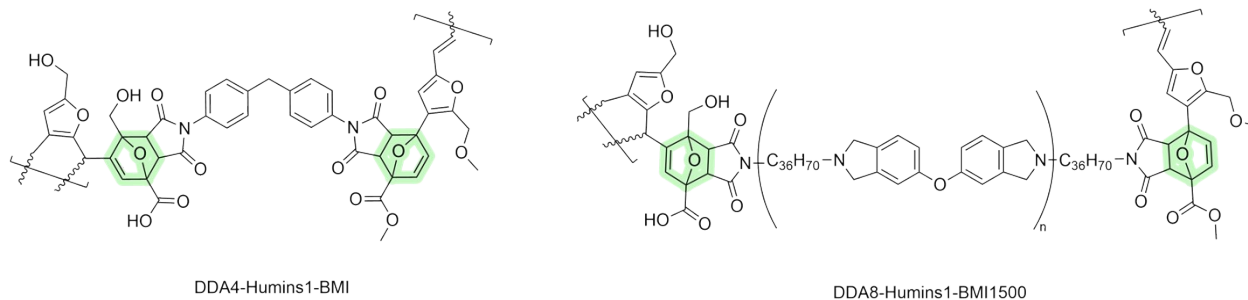


**Figure S37.** Representative structures of DDA4-Humins1 and DDA8-Humins1-BMI1500.

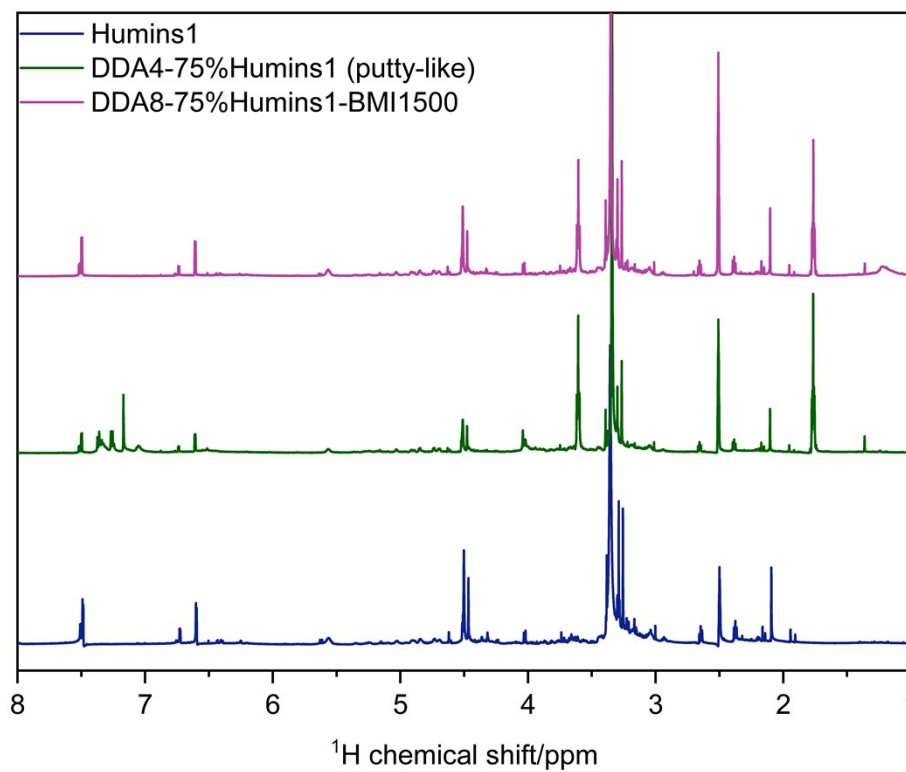


**Figure S38.**  $^1\text{H}$  NMR spectra of DDA8-75%Humins1-BMI1500 with comparison Humins1 and DDA4-Humins1 (putty-like).

**Table S8.** <sup>1</sup>H NMR data for DDA8-Humins1-BMI1500 (600 MHz, DMSO-d<sub>6</sub>, 25 °C)

$\delta$ (ppm)	Multiplicity <sup>1</sup>	Assignment	Comment	$\delta$ (ppm)
~9.95–9.54	br s	Aldehydic/formyl protons (–CHO)	Weak but distinct; typical oxidised humin signatures.	~9.95–9.54
7.49	br m	Aromatic protons	Likely humins' furan-derived aromatic regions.	7.49
6.73–6.00	br m	Furanic/aromatic proton envelope	Central aromatic region of humins.	6.73–6.00
5.56	br m	Conjugated/vinylic proton	Small signal often retained in modified humins.	5.56
4.62–3.57	br m	DA bridgehead/bridge methine & methylene protons	New signals relative to parent humins; diagnostic of DA adduct formation.	4.62–3.57
2.69–2.44	br m	CH <sub>2</sub> adjacent to imide carbonyl (BMI fraction)	Overlaps partially with O–CH <sub>2</sub> of humins.	2.69–2.44
2.04–1.76	br m	Aliphatic CH/CH <sub>2</sub> from humins backbone + DA linkages	Increased intensity vs. unmodified humins.	2.04–1.76
1.36–1.19	br m	Terminal CH <sub>3</sub> / extended aliphatic fragments	Very weak, broad; typical for humins.	1.36–1.19

<sup>1</sup> br s = broad singlet; br m = broad multiplet. Multiplicities are descriptive only; individual spin systems cannot be resolved due to strong broadening and overlap.

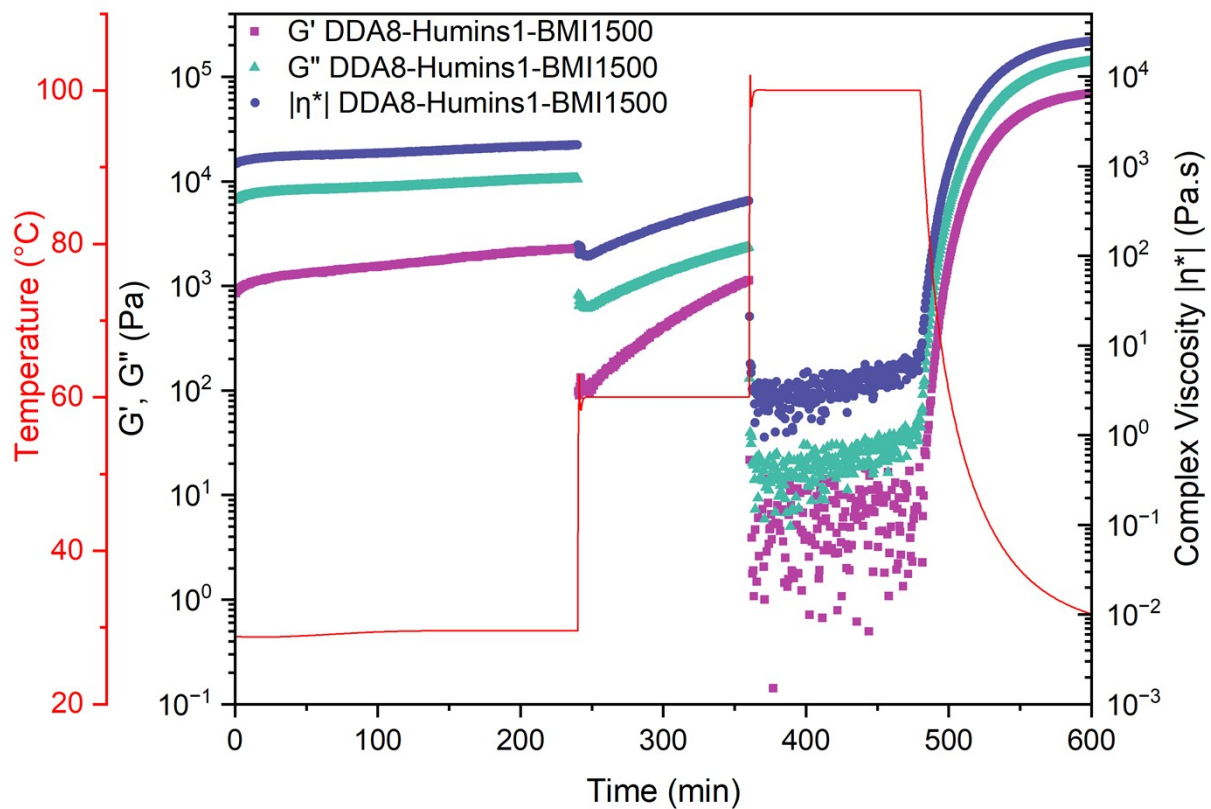


**Figure S39.** Measurements were performed using a 25 mm parallel-plate geometry at  $\gamma = 0.1\%$ ,  $f = 1$  Hz, under a nitrogen atmosphere.

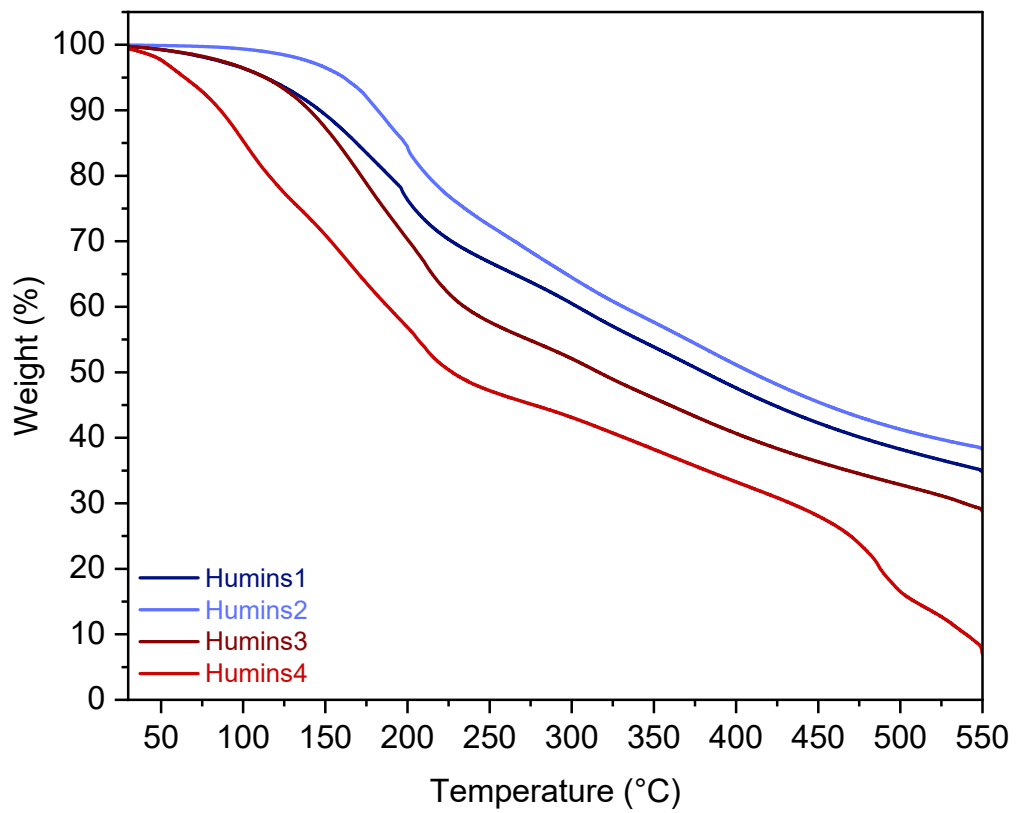


**Figure S40.** TGA curves of different humins samples.

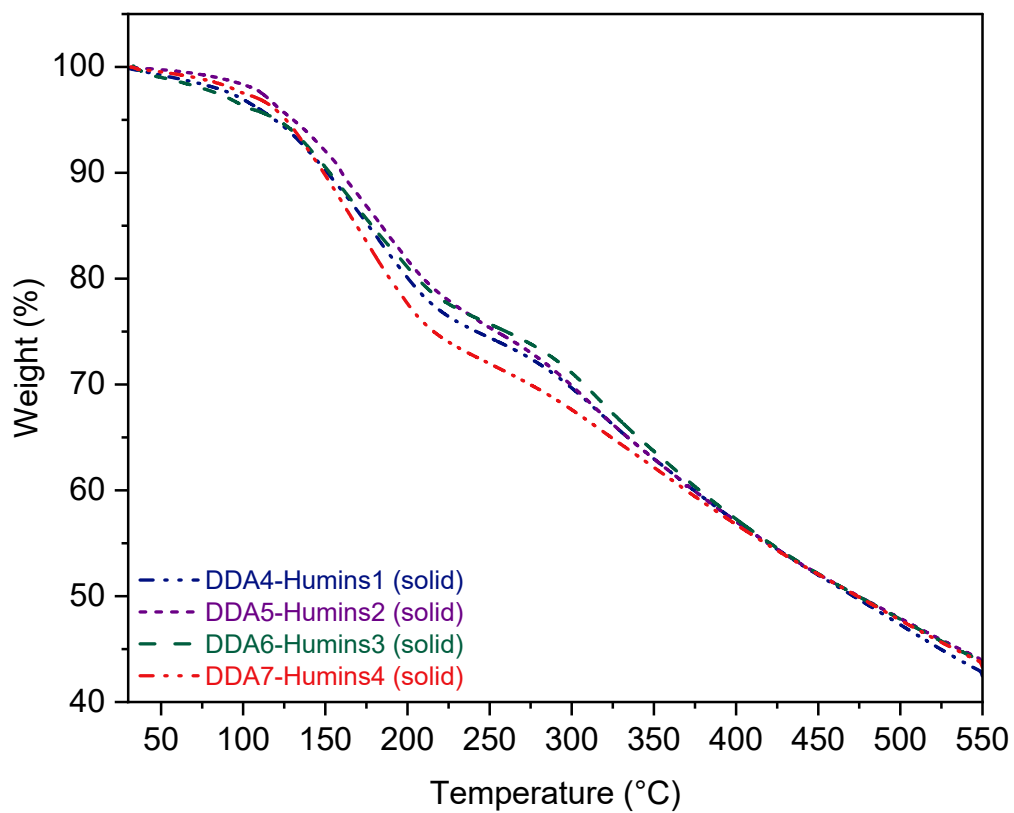


**Figure S41.** TGA curves of solid DDA-humins adducts (DDA4-Humins1, DDA5-Humins2, DDA6-Humins3, DDA7-Humins4).

**Table S9.** Thermal degradation parameters ( $T_{d5\%}$ ,  $T_{50\%}$  and char yield at 550 °C) of humins and their corresponding Diels-Alder adducts.

Sample	$T_{d5\%}$ (°C)	$T_{50\%}$ (°C)	Char yield at 550 °C (%)
Humins1	113.6	380.2	34.7
DDA4-Humins1	119.3	471.7	42.7
Humins2	161.3	409.1	38.2
DDA5-Humins2	104.6	474.6	43.5
Humins3	113.0	316.5	28.7
DDA6-Humins3	120.7	474.3	43.3
Humins4	64.4	227.2	7.0
DDA7-Humins4	126.1	473.9	43.3

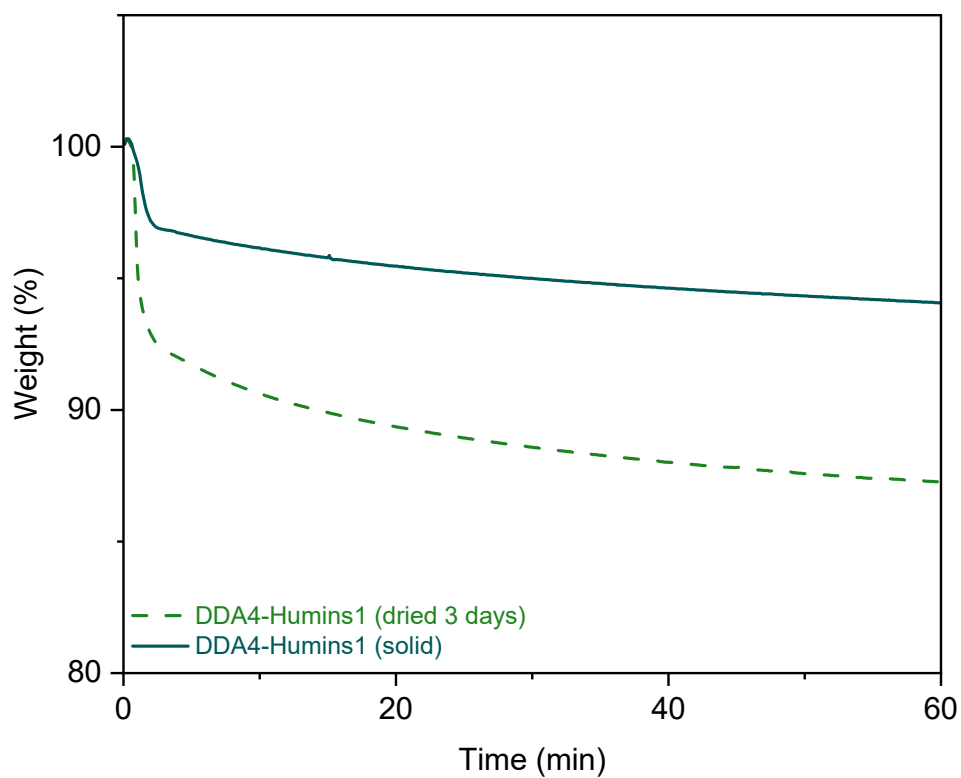


**Figure S42.** TGA curves of DDA4-Humins1 (dried 3 days) and DDA4-Humins1 (solid) samples in isothermal hold at 100 °C.

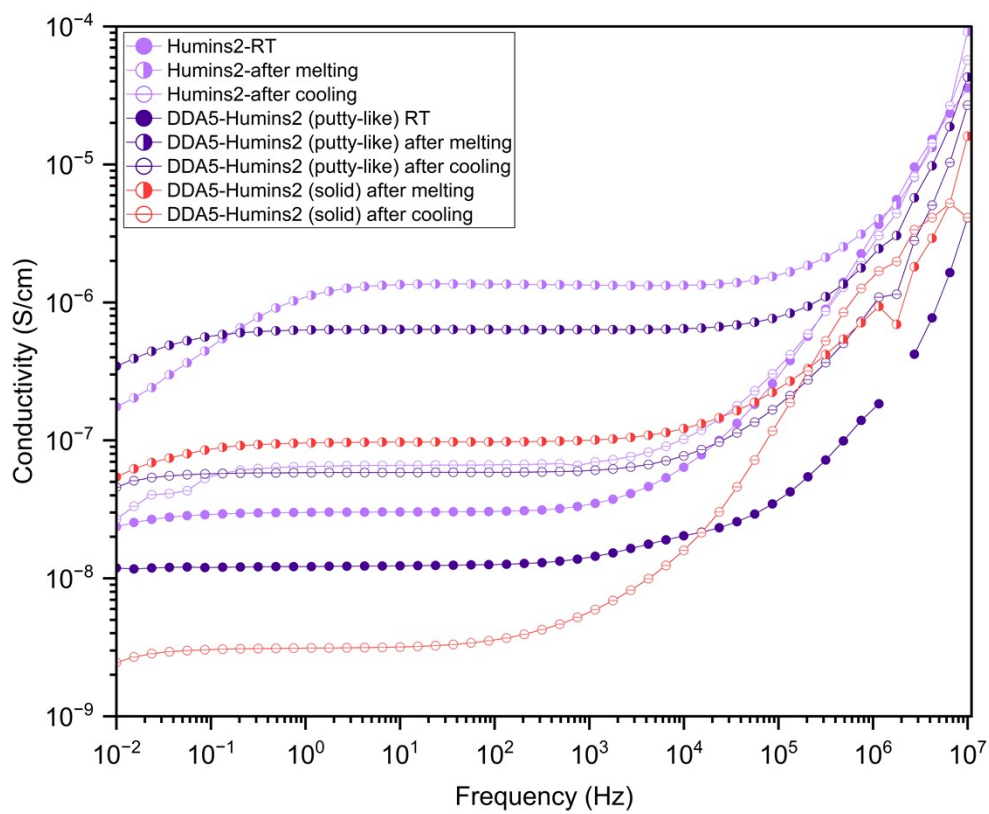


**Figure S43.** Dielectric results: conductivity–frequency plots for Humins2 and DDA5 (putty-like and solid) at room temperature (RT), after melting, and after cooling.

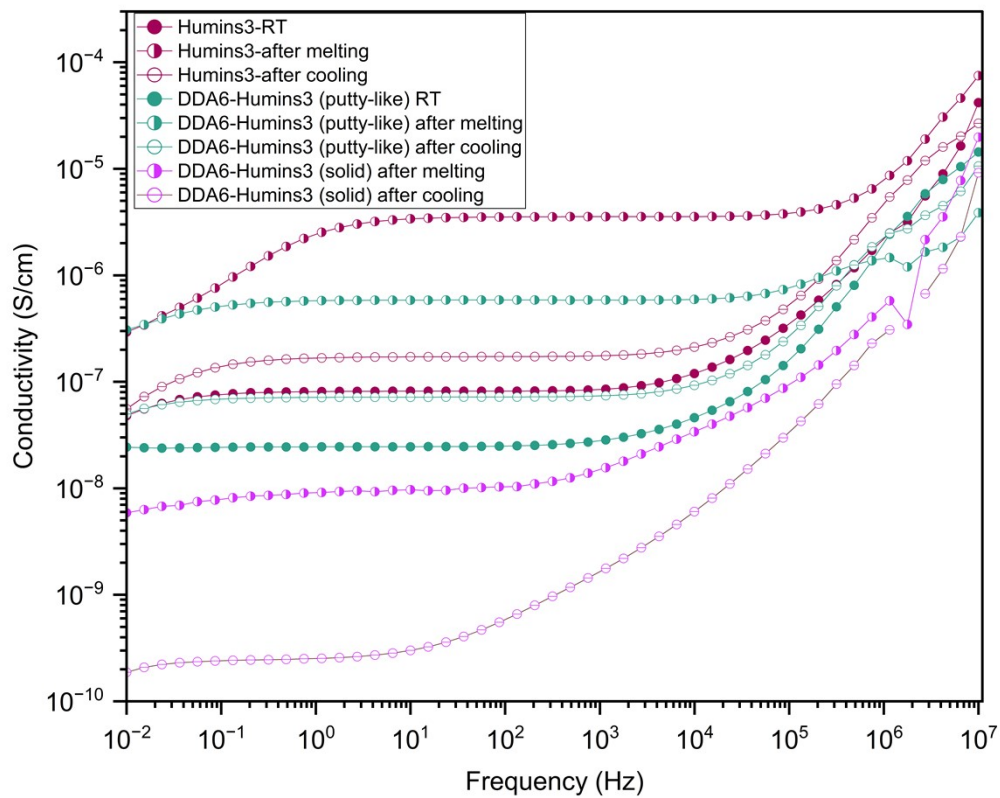


**Figure S44.** Dielectric tests: conductivity–frequency plots for Humins3 and DDA6 (putty-like and solid) at room temperature (RT), after melting, and after cooling.



**Figure S45.** Self-healing behaviour of DDA4 solid on the rheometer plate at 60 °C for 10 minutes.

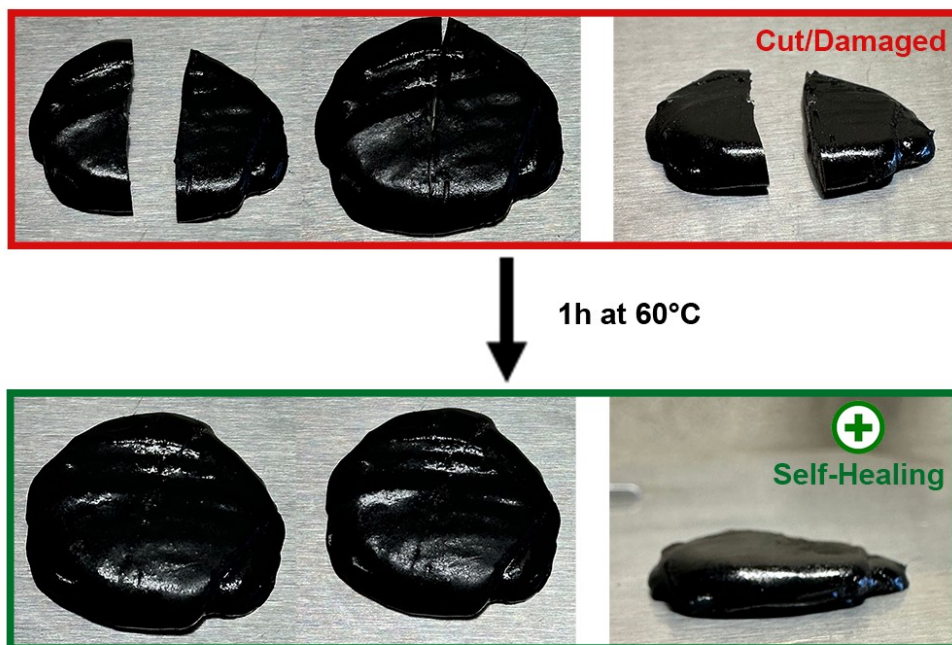


**Figure S46.** Self-healing behaviour of DDA4 solid in the oven at 60 °C for 1 hour.